https://doi.org/10.5194/egusphere-2026-1919
Preprint. Discussion started: 26 May 2026

GCAM-China-v8: An Integrated Global-to-Provincial Framework for Assessing China's Energy and Emission Futures

Shuling Xu[1,31#], Yang Liu[2#], Sha Yu[3#*], Weidong Jia[4], Yongye Jiang[5], Yuqin Li[6], Zeyuan Liu[7], Andy Miller[3], Jianxiang Shen[8], Jingyang Song[1], Can Wang[9], Huaxuan Wang[2], Rui Wang[10], Fan Wu[1], Hongzhi Zhang[11], Mengting Zhu[1], Rongqi Zhu[1], Jenna Behrendt[3], Matthew Binsted[3], Jing Cheng[1], Robert Dahowski[12], Casie Davidson[12], Shiyu Deng[13], Jay Fuhrman[3], Matthew Gidden[3], Chaoyi Guo[3], Jill Horing[14], Hanwoong Kim[15], Chaojun Li[2,16], Bo Liu[17], Xunzhang Pan[18], Pralit Patel[3], Meiyin Qian[19], Yang Qiu[3], Tianming Shao[20], Yisheng Sun[2], Lining Wang[21], Yuyao Yang[22], Brinda Yarlagadda[3], Zihua Yin[23], Jian Zang[24], Qianzhi Zhang[25], Wenjia Cai[8], Wenying Chen[25], Leon Clarke[3], Ryna Cui[3*], Nathan Hultman[3], Bengang Li[5,26], Jiashuo Li[4], Xi Lu[2,27,28,29], Haewon McJeon[30], Bo Wang[9], Can Wang[2], Peng Wang[22], Shuxiao Wang[2], Zhaohua Wang[11], Lixiao Zhang[6], Qiang Zhang[8*], Yang Ou[1,26*]

[1]College of Environmental Sciences and Engineering, Peking University, Beijing 100871, China
[2]State Key Laboratory of Regional Environment and Sustainability, School of Environment, Tsinghua University, Beijing 100084, China
[3]Center for Global Sustainability, University of Maryland, College Park, MD 20742, USA
[4]Institute of Blue and Green Development, Shandong University, Weihai 264209, China
[5]College of Urban and Environmental Sciences, Peking University, Beijing 100871, China
[6]State Key Joint Laboratory of Environmental Simulation and Pollution Control, School of Environment, Beijing Normal University, Beijing 100875, China
[7]School of Public Affairs, Zhejiang University, Hangzhou 310058, China
[8]Department of Earth System Science, Ministry of Education Key Laboratory for Earth System Modeling, Institute for Global Change Studies, Tsinghua University, Beijing 100084, China
[9]School of Management, Beijing Institute of Technology, Beijing 100081, China
[10]Copernicus Institute of Sustainable Development, Utrecht University, 3584 CS Utrecht, The Netherlands
[11]School of Economics, Beijing Institute of Technology, Beijing 100081, China
[12]Pacific Northwest National Laboratory, Richland, WA 99354, USA
[13]The Bartlett School of Sustainable Construction, University College London, London WC1E 7HB, UK
[14]California Energy Commission, Sacramento, CA 95814, USA
[15]Center for Policy Research on Energy and the Environment, Princeton University, Princeton, NJ 08544, USA
[16]Tsinghua Institute for Frontier Interdisciplinary Innovation, Beijing 100084, China
[17]National Renewable Energy Laboratory, Golden, CO 80401, USA
[18]School of Ecology and Environment, Renmin University of China, Beijing 100872, China
[19]Shanghai Academy of Environmental Sciences, Shanghai 200233, China
[20]School of Advanced Manufacturing and Robotics, Peking University, Beijing 100871, China
[21]CNPC Economics and Technology Research Institute, Beijing 100724, China
[22]Institute of Urban Environment, Chinese Academy of Sciences, Xiamen 361021, China
[23]PetroChina International Company Limited, Beijing 100033, China
[24]Tianfu Yongxing Laboratory, Chengdu 610213, China
[25]Institute of Energy, Environment and Economy, Tsinghua University, Beijing 100084, China
[26]Institute of Carbon Neutrality, Peking University, Beijing 100871, China
[27]Institute for Carbon Neutrality, Tsinghua University, Beijing 100084, China
[28]Beijing Laboratory of Environmental Frontier Technologies, Tsinghua University, Beijing 100084, China
[29]Institute for Carbon-Neutrality System Integration Technologies, Tianfu Yongxing Laboratory, Chengdu 610213, China
[30]Graduate School of Green Growth and Sustainability, Korea Advanced Institute of Science and Technology, Daejeon 34141, South Korea

https://doi.org/10.5194/egusphere-2026-1919
Preprint. Discussion started: 26 May 2026

[31]School of Economics and Management, North China Electric Power University, Beijing 102206, China
[#]These authors contributed equally to this work.

Correspondence to: Sha Yu (sha@umd.edu), Ryna Cui (ycui10@umd.edu), Qiang Zhang (qiangzhang@tsinghua.edu.cn), Yang Ou(yang.ou@pku.edu.cn)

Abstract. This paper describes Global Change Analysis Model-China version 8 (GCAM-China-v8), an open-source integrated assessment model that represents interactions among energy, economic, and water systems within a globally consistent framework, with explicit subnational representation for China. GCAM-China-v8 builds on the GCAM and represents the world as 31 geopolitical regions outside China, while disaggregating China into 31 province-level regions to capture regional heterogeneity. GCAM-China-v8 can be used to explore how changes in socioeconomic drivers, technological progress, and policy assumptions affect energy and water demand and production at the subnational level in China, while maintaining consistency with national and international boundary conditions. This paper documents the model structure and data inputs, with particular emphasis on the methodological updates introduced in GCAM-China-v8, including enhanced sectoral and temporal representations. To demonstrate the capabilities of the updated model, we apply GCAM-China-v8 to two illustrative scenarios with contrasting assumptions about future socioeconomic development and energy system transformation. This paper provides a transparent and extensible modeling framework for future research on China's long-term energy and climate transitions. It also contributes to the broader Integrated Assessment Models (IAMs) community by advancing national-scale model development within an open and consistent framework.

1 Introduction

IAMs have become a central tool for assessing long-term transitions of coupled energy, economic, land-use, and climate systems under alternative socioeconomic and policy assumptions (Calvin et al., 2019). While global IAMs have provided critical insights into worldwide mitigation pathways, climate policies are increasingly designed and implemented at the national level (Hultman et al., 2020; Fujimori et al., 2021). National-scale IAMs can better reflect country-specific structures and constraints while preserving consistency with broader global dynamics (Schaeffer et al., 2020; Fujimori et al., 2022). GCAM is widely used as a community model and has a long history of supporting global climate change and energy policy analysis (Ou et al., 2021a). It has been widely used in major international and national assessments such as Intergovernmental Panel on Climate Change (IPCC) reports (2022), in the development and exploration of global scenario frameworks including the Representative Concentration Pathways (RCPs) and Shared Socioeconomic Pathways (SSPs) (Thomson et al., 2011; Clarke et al., 2014; Calvin et al., 2017), and in multi-model intercomparison exercises such as the Energy Modeling Forum (EMF) and ScenarioMIP (Roelfsema et al., 2020; Harmsen et al., 2021; van Vuuren et al., 2025).

To address specific regional research questions, the GCAM community has developed a diverse ecosystem of regional model versions and branches. These adaptations extend beyond the standard 31-region framework and generally fall into two

https://doi.org/10.5194/egusphere-2026-1919
Preprint. Discussion started: 26 May 2026

categories: national models, in which specific countries are newly represented or enhanced with local details, and subregional models, which further disaggregate nations into subnational units such as provinces or states. Examples of national models include GCAM-KSA (Kamboj et al., 2024), GCAM-Chile (Flores et al., 2024), GCAM-Australia (Hassan Niazi, 2025), GCAM-LAC (Yarlagadda et al., 2023), GCAM-CDR (Morrow et al., 2023), GCAM-Ukraine (Diachuk et al., 2025), and GCAM-TU (Zhang et al., 2024a). Subregional variants include GCAM-USA (Iyer et al., 2017), GCAM-China (Cheng et al., 2021a), GCAM-Europe (Sampedro et al., 2025), GCAM-Canada (Younis et al., 2025a), GCAM-Korea (Jeon et al., 2020, 2021a), GCAM-India (Das et al., 2025; Kholod et al., 2021). Among the subregional variants, GCAM-USA serves as the pioneer and has been widely applied to evaluate decarbonization policies and demonstrate substantial heterogeneity across states (Luo et al., 2025; Mongird et al., 2025; Ou et al., 2020; Peng et al., 2021; Zhang et al., 2021).

Building on this growing ecosystem of regional GCAM variants, several research groups have developed China-focused versions of the model to address emerging policy and research questions in China, including GCAM-TU (Shao et al., 2025; Zhang et al., 2024b) and GCAM-AP (Sun et al., 2024). A detailed review of these previous applications is provided in Sect.2.2. While these models have provided valuable insights, existing GCAM family models for China also exhibit several limitations. For instance, many implementations have been developed as project-specific versions based on early versions of the GCAM framework, leading to dated representations in model structure, sectoral coverage, and data conventions. In addition, some variants are not fully open-source or publicly documented, limiting transparency, reproducibility, and extensibility. Data updates are also sometimes inconsistent, with several models relying on outdated base-year calibrations or sector-specific datasets that are not harmonized across the full energy-economy-land system. More importantly, to keep pace with the rapid evolution of China's decarbonization policies, establishing an open-access and community-shared GCAM-China-v8 is imperative to facilitate more efficient, transparent, and reproducible assessments.

In this paper, we present GCAM-China-v8, an open-source integrated assessment model that represents interactions among energy, economic, land, and water systems for China within a globally consistent GCAM framework. GCAM-China-v8 builds on GCAM-v8 architecture and represents China at the provincial level while maintaining consistency with the global energy-economy-land-climate system. The model incorporates updated socioeconomic drivers, expanded sectoral representations, and improved data harmonization to better capture regional heterogeneity and evolving policy contexts in China. By integrating subnational detail with the global GCAM framework, GCAM-China-v8 provides a transparent and extensible platform for analyzing China's long-term energy transitions and climate policy pathways.

The remainder of this paper is organized as follows. Section 2 describes the overall structure of GCAM-China-v8 and its major model components. Section 3 presents illustrative scenario results to demonstrate the model's capabilities. Section 4 discusses key insights, limitations, and directions for future development.

https://doi.org/10.5194/egusphere-2026-1919
Preprint. Discussion started: 26 May 2026

2 Model overview

2.1 Overview of GCAM

GCAM is an open-source, recursive-dynamic integrated assessment model. Structurally, the model core is written in C++ and organized in a modular structure. GCAM represents interactions among multiple systems, including energy, water, land, socioeconomics, and climate. These systems interact through a market-equilibrium framework, in which supply and demand for energy and agricultural commodities are balanced through price-mediated adjustments under exogenously specified socioeconomic assumptions. Spatially, GCAM represents the world as a set of geopolitical regions linked through global markets for tradable goods, including energy carriers, agricultural products, and emissions. Within each region, the model represents energy supply, transformation, and end-use demand across major sectors (electricity, buildings, transportation, and industry), together with coupled land-use and water systems. At the technology level, discrete choice formulations (Clarke and Edmonds, 1993a) are used to represent competition among technologies based on relative costs and performance, reflecting the inertia of real-world transitions. GCAM has been widely used to explore long-term pathways and support global climate assessments. A detailed description of the GCAM framework, equations, and data sources can be found in official documentation and model description papers (Calvin et al., 2019).

2.2 Previous GCAM applications in China

Previous studies using GCAM have examined both sectoral applications and methodological development in China. Application-oriented research in the energy system has focused primarily on the power sector and major end-use sectors, including industry, buildings, and transportation. Methodological studies have extended the GCAM framework through cross-system integrations and model coupling approaches often referred to as “GCAM+”.

Studies using GCAM have examined a wide range of technologies in the power sector in China, including carbon capture and storage (CCS) (Dahowski et al., 2017), bioenergy with CCS (BECCS) (Pan et al., 2018), combined heat and power (Wang et al., 2023b), biomass and coal cofiring (Wang et al., 2024), hydrogen (Zhang et al., 2024c), and direct air carbon capture and storage (DACCS) (Shao et al., 2025). In end-use sectors, previous work has introduced additional sectoral details, including detailed representation of eleven industrial subsectors (Zhou et al., 2013), building-sector disaggregation by four climate zones and three building types (Yu et al., 2014a, b), and transport-sector extension through coupling with the China Transportation Energy Model (Yin et al., 2015a) or the Sectoral Emissions and Energy Demand-Transport Planning Model (SEED-TPM) (Wang et al., 2023a). Despite these developments, many studies still represent China as a single region, limiting the ability to analyze China’s regional heterogeneity. To address this limitation, an early version of GCAM-China was developed in 2019, which disaggregates China into 31 province-level energy-economic systems (Yu et al., 2019). Since then, GCAM-China has been applied to examine provincial energy transitions, such as nuclear power expansion (Yu et al., 2020), coal power retirement (Cui et al., 2021a), and renewables investment (Lou et al., 2025). More recent studies have

https://doi.org/10.5194/egusphere-2026-1919
Preprint. Discussion started: 26 May 2026

used GCAM-China to analyze emerging topics, including transport demand reductions under compact urban development (Fu et al., 2024) and the deployment of DACCS (Kim et al., 2024).

Methodological studies have also focused on extending GCAM through coupling complementary models. One group of studies links GCAM with input-output (IO) models to quantify the socioeconomic and environmental consequences of energy system transitions, such as employment, value chains, and emissions (Peng et al., 2023; Wang et al., 2025a). Other studies couple GCAM with power system optimization models to improve the representation of power system dynamics, including capacity expansion, dispatch constraints, and operational flexibility, especially in the Chinese context (Wang et al., 2025b). In addition, GCAM has been linked with life cycle assessment (LCA) frameworks to evaluate technology-specific environmental impacts, for example, in the assessment of agroforestry biomass power generation in China (Ma et al., 2025).

A growing line of research integrates GCAM-China with air quality and health impact assessment frameworks. A representative example is the Carbon Neutrality and Clean Air synergetic Platform (CNCAP), which combines GCAM-China with the Multi-resolution Emission Inventory for China (MEIC), a dynamic emission projection module (DPEC), and parameterized policy schemes to support assessments of future mitigation pathways (Tong et al., 2020). CNCAP has been applied in multiple studies examining air pollution and associated health impacts under different climate and energy scenarios (Cheng et al., 2021b; Liu et al., 2022; Cheng et al., 2023; Fu et al., 2024; Qin et al., 2024). In addition to CNCAP, other studies integrated GCAM-China into the Air Benefit and Cost and Attainment Assessment System (ABaCAS) to improve the representation of air quality and health impacts (Xing et al., 2020; Sun et al., 2024; Dong et al., 2024).

Table 1 summarizes the main China-focused GCAM-based modeling frameworks and their key methodological features.

Table 1. Summary of previous GCAM applications in China

Model/Framework	Key features	Applications
GCAM-TU (Wang et al., 2016)	Air pollutant emissions control module coupled with end-of-pipe technologies	National energy policies; sectoral mitigation policies; air pollution control
GCAM-TU (Pan et al., 2023)	Detailed end-use sector representations and data update for China	National energy policies; sectoral mitigation policies; technology dynamics
GCAM-TU (Zhang et al., 2024c)	Enhanced hydrogen production, transport, and utilization modules; global hydrogen trade module	Hydrogen technology adoption; international hydrogen trade
GCAM-CHN (Shao et al., 2025)	Calibration to China's 2020 energy consumption and CO_2 emissions; expanded subsector structure and	National energy policies; CCS technologies adoption

https://doi.org/10.5194/egusphere-2026-1919
Preprint. Discussion started: 26 May 2026

	technology portfolio	
GCAM-China (Deng et al., 2025; Kim et al., 2024; Lou et al., 2025; Wang et al., 2025c; Yin et al., 2026; Yu et al., 2019, 2020)	Provincial disaggregation of China; Incorporation of DACCS technologies; Updated solar and wind cost and capacity factors	National and provincial energy policies; power sector technological dynamics
CNCAP (Tong et al., 2020)	GCAM-China with MEIC emission inventory and DPEC emission projection module	Air pollution control policies; health impact assessment
GCAM-China-ABaCAS (Xing et al., 2020)	Coupling GCAM-China with the ABaCAS framework	Air pollution control policies; health impact assessment

2.3 Overview of GCAM-China

GCAM-China-v8 is a version of GCAM that increases the spatial resolution for China to represent subnational provinces. The final calibration year for GCAM-China-v8 is 2021. The model disaggregates the original China region into 31 province-level regions, allowing provincial differences in energy systems, economic activity, and resource endowments to be represented while maintaining consistency with the global GCAM framework. Each region contains representations of key socioeconomic drivers, resource availability, and energy sectors. GCAM-China-v8 represents major supply and end-use sectors, including electricity generation, transportation, buildings, and industry, together with coupled agriculture, land-use, and water systems. Key input data and parameters, such as technology costs, energy intensities, and emission factors, are calibrated using China-specific statistical data and other empirical data. GCAM-China-v8 has been used in a range of studies examining China's long-term energy transition (Cui et al., 2021b), emissions trajectories (Zhong et al., 2025), and policy scenarios (Wang et al., 2026). In this paper, we introduce GCAM-China-v8, which includes a set of data and structural updates to improve the representation of China's evolving energy system and related policy questions. Descriptions of the main model structures, key assumptions, and implementation details are provided in Supplementary Table SM1.

2.4 Socioeconomics

GCAM-China-v8 adopts province-level assumptions on population and economic growth to define the scale of socioeconomic activity in the whole system. These assumptions are aligned with the "middle-of-the-road" Shared Socioeconomic Pathway 2 (SSP2) (O'Neill et al., 2014), ensuring consistency with the Reference scenario assumptions applied to the other 31 global regions in GCAM. Detailed socioeconomic assumptions for the GCAM-China-v8 Reference scenario are provided in Supplementary Table SM2.

https://doi.org/10.5194/egusphere-2026-1919
Preprint. Discussion started: 26 May 2026

The population is treated as an exogenous input to the model. Historical national population data for 1975-2018 are obtained from the China Statistical Yearbook (National Bureau of Statistics of China, 2020) and the China Compendium of 60-year Statistics (National Bureau of Statistics of China, 2009), while provincial population data for 2000-2019 are derived from the Annual National Sample Survey of Population (National Bureau of Statistics of China, 2022). Historical population growth rates are calculated based on these records. Future population trajectories from 2020 to 2100 follow SSP-consistent growth rates applied to the calibrated historical population series (Joint Global Change Research Institute (JGCRI), 2026a).

Historical provincial GDP data are primarily drawn from the China Statistical Yearbook (National Bureau of Statistics of China, 2020) and the China Compendium of 60-year Statistics (National Bureau of Statistics of China, 2009), which are originally reported in units of 100 million RMB. Provincial GDP in the model is expressed in million 2010 USD and is calculated for both historical and future periods based on provincial GDP per capita and population. Historical GDP per capita data for 2010-2019 are obtained from the China Statistical Yearbook (National Bureau of Statistics of China, 2020), with values for 2010-2017 revised to reflect adjustments from the Fourth National Economic Census. All historical GDP figures are deflated to constant 2010 CNY using China-specific GDP deflators from the World Bank World Development Indicators and then converted to 2010 USD using the 2010 average exchange rate of 6.77. GDP per capita for 2019-2021 is projected using growth rates from the World Economic Outlook (International Monetary Fund, 2021), explicitly accounting for the COVID-19 shock in 2020, while long-term projections to 2100 follow growth trajectories from the OECD ENV-Growth or IIASA SSP Database (Shared Socioeconomic Pathways Scenario Database (SSP), 2026).

2.5 Energy

Following GCAM-USA (Joint Global Change Research Institute (JGCRI), 2026b), the energy system of GCAM-China-v8 includes a comprehensive representation of energy production, transformation, distribution, and use for the 31 geopolitical regions outside China and the 31 provinces in China.

2.5.1 Electricity

(1) Electric power supply

The electricity sector in GCAM-China-v8 is represented as an energy transformation sector that converts primary fuels (e.g., coal, gas, oil, bioenergy) into electricity through a portfolio of competing generation technologies. Provincial electricity generation by fuel and technology is calibrated using data from the China Electric Power Statistical Yearbook (China Electricity Council, 2021). Consistent with the GCAM power sector module (Eurek et al., 2017; Muratori et al., 2017a; Kyle et al., 2021), each electricity technology is specified by region-specific logit exponents, share weights and interpolation rules, and input-output coefficients, together with cost and performance assumptions. Technology competition is implemented through discrete technology vintages whose market shares respond to generalized costs, which reflect (i) exogenous non-fuel costs (capital and operations and maintenance), (ii) endogenous fuel costs determined by fuel prices and conversion

https://doi.org/10.5194/egusphere-2026-1919
Preprint. Discussion started: 26 May 2026

efficiencies, and (iii) policy-driven emissions costs (Muratori et al., 2017a). End-use sectors determine annual electricity demand through technology and fuel choices in response to service demands and energy prices; the electricity sector meets this demand through market clearing, linking generation, trade, and prices within the modeled supply chain. Building on the electricity-sector structure in the GCAM-USA implementation (Chini et al., 2018), GCAM-China-v8 adopts a similar load-segmentation framework. Annual electricity demand is decomposed into four horizontal generation segments (baseload, intermediate, subpeak, and peak) at the province level, and four corresponding vertical demand segments at the grid-region level. Horizontal-to-vertical coefficients, computed from demand fractions and time fractions for each of China's six electricity grid regions, govern how generation from technologies operating at different capacity-factor tiers is allocated to the vertical demand segments.

(2) Electricity trade

Moreover, to represent China's inter-provincial transmission in a way that is consistent with the net-trade-balance framework, GCAM-China-v8 also introduces a grid electricity trade layer that adapts the "gross electricity trade" concept developed for GCAM-USA (Chini et al., 2018). The trade is represented at the province level to reflect the underlying transmission geography, and the resulting provincial trades are integrated into the six electricity grid regions embedded in GCAM-China-v8. Provincial electricity flows are calibrated to the model base year using historical values from the Compilation of Statistical Data of Electric Power Industry (China Electricity Council, 2005), covering 2005-2021. Specifically, a trading region can simultaneously import and export electricity within a model period: gross imports and exports are derived from an underlying net trade quantity using an empirically informed import-to-export ratio that controls the intensity of two-way exchanges. In GCAM-China-v8, each province is treated as a trading region whose electricity balance can be met by local generation and net imports, while gross flows are computed to better reflect bidirectional transfers observed in real transmission networks. Electricity trade, therefore, allows provincial load-segment demands to be satisfied through a combination of local generation and interregional exchanges.

(3) Disaggregation of coal power technologies by vintage

To capture heterogeneity in China's coal-fired fleet, we explicitly disaggregate coal-fired power generation technologies in GCAM-China-v8 by construction vintage. Specifically, coal-fired units operating in 2021 at the provincial level are subdivided into multiple vintages (before 1990, 1991-1995, 1996-2000, 2001-2005, 2006-2010, 2011-2015, 2016-2021). Each vintage represents units commissioned within a given time window, reflecting differences in technical characteristics and remaining operational lifetimes, with older vintages generally subject to earlier retirement. The allocation of generation across vintages at the provincial level is calibrated using historical generation data from the Multi-resolution Emission Inventory for China (MEIC) (Zheng et al., 2018). MEIC provides province-level coal generation by plant age, which is used to split the total 2021 coal output across vintage-specific technologies within each province.

https://doi.org/10.5194/egusphere-2026-1919
Preprint. Discussion started: 26 May 2026

2.5.2 Industry

The industrial sector in GCAM-China-v8 represents a substantial extension of the standard GCAM framework. Figure 1 presents the detailed structure of the industrial sector in GCAM-China-v8, including 10 service types, 8 fuels & feedstocks, and 19 technologies. Final demands for industrial energy services are represented at the provincial level, utilizing GDP-driven demand functions adapted from GCAM but with expanded sectoral coverage from a variety of data sources. Beyond the conventional GCAM industrial categories of cement and nitrogen fertilizer, GCAM-China-v8 incorporates explicit representations of iron and steel production, coking, chemicals, and energy consumption from non-road machinery used in agriculture, construction, and mining activities.

Industrial demands are characterized by two distinct specification approaches that reflect data availability and sectoral characteristics. For iron and steel and coking sectors, demands are expressed as physical production quantities (million tons) derived from provincial-level statistics published in the China Industrial Statistical Yearbook (2026) by the National Bureau of Statistics of China (NBSC). For other industrial subsectors, demands are represented as energy service requirements, with base-year energy consumption primarily sourced from the Multi-resolution Emission Inventory for China-High Resolution (MEIC-HR) (Zheng et al., 2017, 2021), which provides facility-level estimates based on bottom-up surveys. To maintain international consistency, sectoral total energy consumption is reconciled with IEA Energy Balances, with province- and sector-specific scaling factors applied when MEIC-HR facility-level data exceed IEA sectoral totals.

For each industrial product, GCAM-China-v8 represents the production, demand, and net trade structure, with separate formulations of demand and supply competition. National-level demands for physical products (iron and steel, cement, fertilizer, coke) are determined by macroeconomic drivers and sectoral consumption following the demand formulation described by van Ruijven et al. (2016), while demands for energy-intensive industrial services follow the standard industrial energy service approach. Provincial production competes to supply these national demands based on their production costs, which reflect local fuel prices, technology portfolios, and carbon constraints. Historical provincial production shares are used for base-year calibration, with future production allocation determined endogenously through a logit-based competition mechanism (Mcfadden, 1974).

The technological representation includes both conventional and low-carbon production technologies, with technology competition following the discrete choice framework described by Clarke and Edmonds. (1993b). For iron and steel, the model explicitly represents conventional production technologies (such as blast furnace-basic oxygen furnace routes and electric arc furnace scrap-based production) alongside low-carbon technologies (such as hydrogen-based direct reduced iron and CCS-equipped facilities). Similar technology portfolios are specified for cement, chemicals, and other subsectors. Technologies compete for market share based on levelized production costs, including non-energy investment, operating

https://doi.org/10.5194/egusphere-2026-1919
Preprint. Discussion started: 26 May 2026

expenses, fuel costs, and carbon prices where applicable. Provincial-level calibration reflects differences in industrial structure, technology vintages, energy prices, and resource endowments across provinces. Key technological and economic parameters for each industrial subsector, including elasticity parameters, input feedstock, and cost assumptions, can be seen in Supplementary Table SM3.

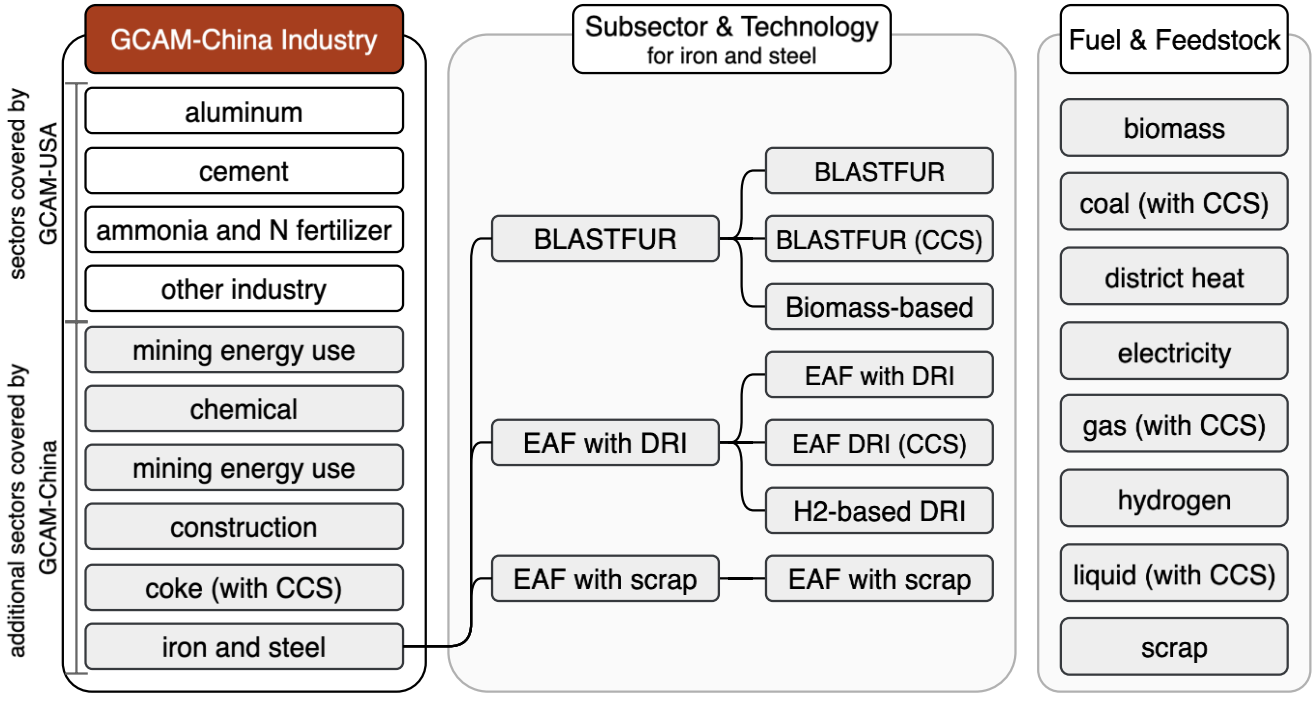

Figure 1: Structure of the industrial sector in GCAM-China-v8.

2.5.3 Building

GCAM-China-v8 includes detailed energy services and technology choices represented in the China building sector. Within each province, the residential building energy demand is disaggregated from a single, representative consumer into 20 consumer groups, differentiated by income deciles and the urban-rural differences in modern technology access. The decile groups are ordered from lower income (d1) to higher income (d10). Income levels for these deciles are exogenous inputs, derived from provincial income distribution projections following the methodology of Casper et al. (2023) and Narayan et al. (2023). Key input data include provincial Gini coefficients calculated from the China Statistical Yearbooks (National Bureau of Statistics, 2016), national Gini projections for 2015-2060 (Rao et al., 2019), and population and urbanization projections (Chen et al., 2020).

The modeling of residential demand begins with estimating per-capita floorspace using a Gompertz function. This function relates per-capita living space to income and population density and reflects physical limits to building expansion, as shown

https://doi.org/10.5194/egusphere-2026-1919
Preprint. Discussion started: 26 May 2026

in Eq. (1). Higher population density effectively lowers the maximum potential floorspace per person. Because per capita GDP is the main driver of per capita floorspace demand and there is no building vintaging in the model, a reduction in per capita GDP directly implies a reduction in per capita floorspace. To prevent this, the model imposes a constraint on floorspace for each consumer group, so that it does not fall below its final calibration year level regardless of future income fluctuations.

$$f_{p,r,t,i} = (UnadjSat_p - \alpha \times \log(PD_{p,t})) \times \exp(-\beta \times exp(-\gamma \times \log(GDPpc_{p,r,t,i}))) + k_{p,r} \quad (1)$$

where $f_{p,r,t,i}$ denotes per-capita floorspace demand in province p, spatial context r (urban/rural areas), year t, and income group i. *UnadjSat* represents the unadjusted satiation level, defined as the maximum potential per capita floorspace demand, which is adjusted based on the provincial population density $PD_{p,t}$ (population divided by habitable land). Income heterogeneity is captured through group-specific per-capita GDP $GDPpc$. *UnadjSat*, α, β, γ are parameters consistent with Sampedro et al. (2024), and $k_{p,r}$ is the bias term calibrated from province-level data.

Energy services are categorized into thermal activities, such as space heating and cooling, and non-thermal activities, including hot water and cooking, lighting, and appliances. The demand for these services, expressed as intensity per unit of floorspace, depends on demographic shifts, building characteristics, and economic factors. Thermal demands are particularly sensitive to climate conditions, represented by heating and cooling degree days, as well as the thermal efficiency of the building shell. Non-thermal services are primarily influenced by rising income levels and population growth. The model also accounts for internal heat gains from non-thermal equipment, which partially offsets the energy required for space heating, as shown in Eq. (2) and Eq. (3).

$$E^{thermal}_{p,r,t,i} = k_{p,r} \times \left(\Delta T_{p,t} \times \eta_{p,r,t} \times R_{p,r} - \lambda_{p,r} \times IG_{p,r,t,i}\right) \times \left[1 - \exp\left(-\frac{ln(2)}{\mu_{p,r}} \times \frac{GDPpc_{p,r,t,i}}{P_{p,r,t}}\right)\right] + bias_{p,r} \quad (2)$$

$$E^{non-thermal}_{p,r,t,i} = k_{p,r} \times \left(1 - \exp\left(-\frac{ln(2)}{\mu_{p,r,C}} \times \frac{GDPpc_{p,r,t,i}}{P_{p,r,t}}\right) + bias_{p,r}\right) \quad (3)$$

where $E^{thermal}_{p,r,t,i}$ denotes per-floorspace demand for modern heating and cooling in province p, spatial context r (urban/rural areas), year t, and income group i. $E^{non-thermal}_{p,r,t,i}$ denotes per-floorspace demand for non-thermal energy activities. k is the unadjusted satiation level of residential service demand, assumed to be identical across income groups and adjusted according to thermal load. ΔT represents heating degree days (HDD) or cooling degree days (CDD). η is the building shell conductivity, representing the thermal efficiency of building envelopes. R is the ratio of floorspace to building area. IG represents internal heat gains from non-thermal services, scaled by the factor λ. The adjusted satiation level of service

https://doi.org/10.5194/egusphere-2026-1919
Preprint. Discussion started: 26 May 2026

demand is defined as the base-year energy service consumption per floorspace multiplied by a factor ranging from 1.01 to 1.20, depending on the activity type. The transition toward the satiation threshold is calibrated by μ, reflecting the affordability ratio of per-capita GDP to service price (P). $bias$ is the bias adder, defined as the difference between estimated and actual province-level demand.

Functional forms for both floorspace and energy services are first calibrated at the provincial aggregate level. This calibration follows the approach used in GCAM (Sampedro et al., 2022, 2024) and GCAM-USA (Zhang et al., 2025). Provincial energy data from the China Building Energy and Emissions Database (Yu et al., 2024) are used to calibrate energy consumption by fuel type. Additionally, GCAM-China-v8 includes more technological details in the building sector than in the previous version, including 57 representative technologies. As in the core GCAM, building services in GCAM-China-v8 are represented by a two-level nested logit structure, where technologies (e.g., conventional and high-efficiency gas furnace) compete within subsectors (e.g., gas, electricity, liquid fuels) to supply specific services.

2.5.4 Transportation

In GCAM-China-v8, the transportation sector mirrors the structure of the core GCAM model (Mishra et al., 2013), with a detailed representation of subnational energy and service demand. This sector is organized into four final demands: passenger travel, freight, long-distance passenger air, and international freight shipping. Passenger travel includes domestic aviation, high-speed and conventional rail, buses, two- and three-wheelers, and light-duty vehicles. Light-duty vehicles are further disaggregated by three size classes and specific technologies (liquid internal combustion engines, natural gas, hybrid electric, battery electric, and fuel cell electric). Similarly, freight covers domestic shipping, freight rail, and trucks (light-, medium-, and heavy-duty), which are also explicitly differentiated by specific technologies (oil, natural gas, biomass liquids, hydrogen, and electricity). The demand D for transportation services (e.g., passenger-km, tonne-km) is given by Eq. (4).

$$D_{p,t} = D_{p,t-1} \times \left(\frac{GDPpc_{r,t}}{GDPpc_{r,t-1}}\right)^{\theta} \times \left(\frac{P_{r,t}}{P_{r,t-1}}\right)^{\mu} \times \left(\frac{N_{r,t}}{N_{r,t-1}}\right) \quad (4)$$

Where P is the total service price aggregated across all modes, N is the population, and θ and μ are income and price elasticities, respectively. Mode competition at the subsector level accounts for the value of travel time, as reflected in the generalized cost Eq.(5).

$$P_{m,p,t} = \frac{W_{p,t} \times \delta_{m,p,t}}{S_{m,p,t}} + \sum_{j} \left(S_{j,m,p,t} \times P_{j,m,p,t}\right) \quad (5)$$

Where W is the wage rate ($/hour) calculated from the per capita GDP, V is a unitless parameter representing the cost associated with travel expressed as a multiplier of the wage rate (value of time, or VOT). δ is the average door-to-door speed

https://doi.org/10.5194/egusphere-2026-1919
Preprint. Discussion started: 26 May 2026

of mode m (KM/hour). $S_{j,m,p,t}$ and $P_{j,m,p,t}$ is the share and cost of technology j in mode m, province p, and year t. Technology costs are calculated using Eq. (6).

$$P_{j,m,p,t} = \frac{P_{f,p,t} \times EI_{j,m,p,t} + NP_{j,m,p,t}}{L_{j,m,p,t}} \quad (6)$$

Where $P_{f,p,t}$ is the fuel price, EI is the vehicle energy or fuel intensity, NP is the non-fuel price, and L is the load factor defined either as passengers per vehicle or tonnes per vehicle. Several previous studies using GCAM have analyzed long-term mitigation pathways and macro-level technology adoption at the global scale (Bosetti and Longden, 2013; Kyle and Kim, 2011; Speizer et al., 2024) and the specific regions (Kholod and Evans, 2016; Ou et al., 2021b; Wu et al., 2022; Yin et al., 2015b). Additionally, targeted studies have investigated the unique decarbonization challenges in specific sub-sectors like freight (Muratori et al., 2017b) and public rail (Chaturvedi and Kim, 2015), while multi-model comparisons have been conducted to assess structural uncertainties across different modeling frameworks (Girod et al., 2013; Paladugula et al., 2018; Yeh et al., 2017).

2.5.5 Resource

Primary energy resources are modeled using exogenous supply curves that prescribe resource availability as a function of the energy price. Primary energy supply of depletable resources, including coal, oil, natural gas, and uranium, is represented at the national level, using the same resource supply curves for extraction costs and resource availability as in the global GCAM. These depletable resources are represented as cumulative resource quantities (in EJ), which are drawn down in each time period as each resource is consumed. Renewable resource supply curves are represented as annual resource quantities (in EJ/yr). The supply of utility-scale solar photovoltaic (PV) and onshore wind is represented at the provincial level, while other renewable technologies, such as distributed solar, concentrated solar power, geothermal, and hydropower, are represented at the national level.

We updated the provincial resource supply curves for utility-scale solar PV and onshore wind power. Unlike some previous GCAM versions that treated utility-scale solar PV as an unlimited resource, GCAM-China-v8 adds a resource curve for utility-scale solar PV and updates the parameters for the onshore wind power resource curve based on recent high-resolution assessments of resource potential in China (Lu et al., 2021; Chen et al., 2024). These studies estimate technically developable solar and wind potential in 10 km × 10 km grid cells, considering site-specific constraints such as solar irradiance, wind speeds, terrain, and land-use restrictions. Grid-cell levelized cost of electricity (LCOE) is then used to construct provincial renewable energy resource supply curves using the Eq. (7):

$$Q = MaxResource \times \frac{P^{CurveEx}}{(MidPrice^{CurveEx} + P^{CurveEx})} \quad (7)$$

https://doi.org/10.5194/egusphere-2026-1919
Preprint. Discussion started: 26 May 2026

where Q denotes the quantity of electricity produced, and P denotes the price. These two variables are endogenously determined within GCAM-China-v8, while the remaining parameters are exogenous to shape the supply curves. $MaxResource$ represents the maximum available quantity of renewable energy production at any price (in EJ), $MidPrice$ represents the price at which half of the $MaxResource$ is produced (in \$/kWh, converted to \$/GJ internally), and $CurveEx$ is a unitless shape parameter. $CurveEx$ is calibrated using grid-cell-level Q (electricity generation potential) and P (LCOE) data from previous studies (Lu et al., 2021; Chen et al., 2024), which are used to construct provincial renewable supply curves.

2.5.6 Biomass

Following GCAM-USA, GCAM-China-v8 further disaggregates bioenergy production and consumption to the provincial level (Javadi et al., 2024). For biomass resource supply, crop residues and purpose-grown energy crops are estimated at the basin level and aggregated to the national level as raw biomass supply (referred to as regional biomass in GCAM). During the processing of regional biomass resources into delivered biomass, the model further disaggregates the resources to the provincial level based on the historical production data for corn ethanol and biodiesel refining products (Asia-Pacific Economic Cooperation (APEC), 2015).

Delivered biomass is converted through 21 technologies and consumed by 5 final sectors at the province level, as shown in Table 2, including power, refining, heat, industry, and building sectors (Calvin et al., 2014). Each province first meets its demand using domestically supplied biomass, and when local supply is insufficient, additional biomass is drawn from the national resource pool. Among the 21 conversion technologies, eight are bioelectricity technologies with and without carbon capture technologies, eight are refining technologies that convert biomass resources into biodiesel, ethanol, Fischer-Tropsch biofuels, two are biohydrogen conversion technologies, and the remaining take biomass-based feedstocks as inputs for district heating, iron and steel production, and other industrial energy uses. The adoption of bioenergy technologies follows the standard GCAM technology competition framework based on relative costs and carbon prices. Technology parameters are assumed to be uniform across provinces and follow national trends.

Table 2. Bioenergy conversion flows from resource, technology, to demand

Supply	Conversion technology	Demand
Agricultural Residues,	Biomass_base_conv (CCS)	Power
	Biomass_base_IGCC (CCS)	Refining
Purposed-grown biomass	Biomass to H_2 (CCS)	
	FT biofuels level1 (CCS)	Heat
	FT biofuels level2 (CCS)	Industry
Manure, sewage sludge, and municipal solid waste	Cellulosic ethanol1 (CCS)	Building

https://doi.org/10.5194/egusphere-2026-1919
Preprint. Discussion started: 26 May 2026

Cellulosic ethanol 2 (CCS)
Biodiesel (CCS)
Wood furnace
Biomass cogeneration
Biomass gasification

2.6 Emissions

2.6.1 Direct Air Carbon Capture and Storage

The parametrization and market structure for DACCS in GCAM-China-v8 follow (Fuhrman et al., 2020, 2023), which first implemented DACCS in the global, 31-region version of GCAM. In the default configuration, DACCS is characterized by high costs and energy inputs per tonne of CO_2 removed in the present day, with moderate improvement through 2050. Model users can specify alternative cost and performance trajectories, in which DACCS costs and energy requirements either remain high or decline more rapidly by mid-century. The implementation of DACCS at the provincial scale in China follows (Kim et al., 2024), which scales the maximum deployment potential in each province according to its share of onshore geological carbon storage relative to the national total. Based on stakeholder feedback that high-temperature DACCS processes using natural gas for solvent regeneration are unlikely to be deployed in China, this technology is excluded by assigning a share-weight of zero.

2.6.2 Non-CO_2 greenhouse gas emissions

We extend GCAM-China-v8 to represent non-CO_2 greenhouse gas emissions (CH_4 and N_2O) from energy end-use sectors at the provincial level, consistent with the national non-CO_2 accounting in the core GCAM framework. In GCAM-China-v8, sectoral emissions are computed as the product of activity levels and emission factors that vary over time and across scenarios to reflect changes in technology and pollution-control policies. At the national scale, CH_4 and N_2O emission inventories and emission-factor trajectories for China follow the standard GCAM non-CO_2 emissions module, with anthropogenic CH_4 and N_2O emissions initialized from the Community Emissions Data System (CEDS), following the methodological framework described by Hoesly et al. (2018). GCAM disaggregates national road-transport CH_4 and N_2O using GAINS emission factors by transport mode (passenger, freight) and fuel. Within this framework, we disaggregate China's energy-related CH_4 and N_2O emissions across 31 provinces using province-specific energy inputs or service outputs, while keeping the national non-CO_2 representation unchanged. The same data pipeline also supports the evaluation of enduse-related fluorinated gases (HFCs, PFCs, and SF_6) using analogous activity-emission-factor relationships; however, given limitations in technology- and province-resolved inventories, a full provincial assessment of HFCs, PFCs, and SF_6 is not included in this version.

https://doi.org/10.5194/egusphere-2026-1919
Preprint. Discussion started: 26 May 2026

For the transport sector, we construct national, technology-specific historical emission factors for CH_4 and N_2O (kg per unit of useful energy) using the core GCAM energy-emissions inventories and calibrated transport energy inputs. These emission factors are calculated separately for on-road and off-road modes and for each fuel. The resulting time-varying coefficients are applied uniformly across provinces, such that provincial emissions scale with fuel consumption by mode and fuel, while the sum across provinces matches the national transport emissions trajectory.

For buildings, fertilizer production, and other industrial energy use, we allocate national CH_4 and N_2O emissions to provinces based on their share of sectoral final energy input in GCAM-China-v8. National emissions by sector, fuel, and year are taken from the core GCAM data system. Emissions in province p for sector s and year t are given by Eq. (8):

$$E_{p,s,t} = \frac{EI_{p,s,t}}{\sum_{p'} EI_{p',s,t}} \times E_{China,s,t} \quad (8)$$

Where $EI_{p,s,t}$ denotes provincial final energy input and $E_{China,s,t}$ denotes the corresponding national emissions. This formulation assumes spatially homogeneous emission factors within each sector-fuel combination, while allowing provincial emissions to differ through variations in energy structure and demand.

Refining-sector CH_4 and N_2O emissions are treated analogously, with technology- and time-dependent emission factors consistent with the national refinery representation. Resource extraction and agricultural non-CO_2 sources, which dominate China's total CH_4 and N_2O emissions, remain represented at the national or basin level and are not yet disaggregated in this version.

2.7 Water

GCAM-China-v8 represents water supply and demand endogenously at the subnational scale. Water resource availability and sectoral demands are resolved through a water market mechanism (Joint Global Change Research Institute (JGCRI), 2026c), in which water prices increase as demand approaches resource limits.

Water supply is represented from three freshwater sources: renewable water (surface and ground), non-renewable (fossil) groundwater, and desalinated water. Seawater is treated as an unlimited resource for cooling thermal power plants in coastal provinces. All water resources are characterized at the HUC-2 river basin level, with source-specific extraction costs and availability constraints. China's water system is represented by 22 river basins (Supplementary Table SM4**)**, some of which are shared with neighbouring regions, such as Mongolia, Russia, and India. Detailed descriptions of the GCAM water supply and market mechanisms can be found in Kim et al. (2016) and Turner et al. (2019).

Water demand is tracked endogenously across all sectors in terms of both water withdrawal and consumption. Withdrawal refers to the total volume of water extracted from the supply system, while consumption represents the fraction not returned

https://doi.org/10.5194/egusphere-2026-1919
Preprint. Discussion started: 26 May 2026

for immediate reuse. Water demand drivers (activities) are modeled at multiple spatial scales and mapped to the province level.

Several sectors, including electricity generation, manufacturing, and municipal water use, are represented directly at the provincial level. For municipal water use, province-specific water demand coefficients are calculated using historical water withdrawal data from China's Water Resources Bulletin (Ministry of Water Resources of the People's Republic of China, 2021). Municipal demand is driven by provincial socioeconomic trends, while the withdrawal-to-consumption ratio is assumed to improve at a constant rate over time across provinces.

Manufacturing water demand coefficients for specific sectors (iron and steel, cement, chemicals, and coke) are derived from industrial water-use quotas issued by the Ministry of Water Resources of China and further calibrated using historical province-level manufacturing water use data (Ministry of Water Resources of the People's Republic of China, 2021). These coefficients are held constant over time, so future industrial water demand depends on projected activity levels.

For the power sector, water withdrawal and consumption coefficients are specified by fuel, generation technology, and cooling system based on Macknick et al. (2012). These coefficients are combined with province-level cooling technology shares derived from a national power plant database to estimate average water-use coefficients by technology and fuel. The resulting coefficients are calibrated using historical thermal power water use data from Zhou et al. (2020).

Three additional sectors, primary energy extraction (mining), agriculture (irrigation), and livestock, are not represented at the province level. Their water demands are driven by national activity (energy and livestock) or land-use regions (irrigation). Water demand coefficients for these sectors are calibrated using historical total water use data from China's Water Resources Bulletin (Zhou et al., 2020), following Calvin et al. (2019) and Graham et al. (2021). These demands are then downscaled to provinces using sector-specific historical demand shares derived from 0.5° × 0.5° gridded water demand data (Huang et al., 2018).

Province-level water demands are aggregated to the river basin level, where water supply and demand are balanced. Province-to-basin mappings (Supplementary Table SM4) follow Huang et al. (2018) and are fixed at 2010 values, so future inter-basin competition reflects historical spatial demand patterns.

2.8 Example of an incentive policy for nuclear electricity generation

In addition to policy interventions such as carbon pricing (Huang et al., 2023) and emissions constraint (Fuhrman et al., 2023) implemented in the core GCAM, GCAM-China-v8 allows for province-level policy specification. One approach is to define provincial scalars for exogenous shutdown deciders (Matthew Binsted et al., 2023), which control the deployment of

https://doi.org/10.5194/egusphere-2026-1919
Preprint. Discussion started: 26 May 2026

vintages. These scalars represent the maximum share of a given vintage that can remain in operation. The output can be scaled above or below the technology vintage's original output. A scalar between 0 and 1 phases out existing vintages (e.g., fossil-based electricity generation or blast furnaces in steelmaking), whereas a scalar greater than 1 maintains or expands their deployment (e.g., renewable-based electricity generation). For example, a scalar of 0.7 for a coal-based electricity generation vintage from 2015 indicates that 30% of this capacity is retired in the corresponding model period.

As a hypothetical example for demonstration, we implement policy interventions that promote nuclear electricity generation. Scalars for exogenous deciders are specified for nuclear capacity deployed in 2021 in Shandong, Fujian, Zhejiang, and Guangdong, which are major nuclear power provinces in China, reflecting near-term policy support for nuclear development. The 2021 vintage is used as the baseline, and a uniform scalar is applied across these provinces based on national capacity targets. National nuclear capacity is 53.26 GW in 2021 (Kang et al., 2022) and is projected to reach 70 and 200 GW in 2025 and 2040 (China Nuclear Energy Association, 2025). This corresponds to scalars of 1.31 for 2021-2035 and 3.75 for 2040-2060.

3 Results

This section presents results for two scenarios: a Reference (REF) scenario and a Carbon Neutrality (CN) scenario. We report model outputs for energy, emissions, water, and an example of nuclear policy interventions, and comparisons with historical data. These scenarios illustrate model behavior and consistency under different transition conditions.

3.1 Energy

3.1.1 Electricity

(1) Electricity generation mix

Figure 2 illustrates the transformation of power generation under the REF and CN scenarios. Both scenarios show rising electricity generation in the short to medium term, increasing from 30.8 EJ in 2021 to 41.0 EJ in 2035, reflecting growing electrification and economic growth. Thereafter, the pathways diverge: generation in REF peaks around 2050 at 46.3 EJ and declines to 45.1 EJ by 2060, while CN continues to expand to 49.8 EJ by 2060, driven by broader electrification in end-use sectors.

The REF scenario shows limited structural change in the power sector. Unabated coal remains dominant, declining from 63% in 2021 to 36% in 2060, while remaining the largest generation source. Gas-fired generation increases to 1.4 EJ by 2060. Wind and solar expand from 11% to 43% over 2021-2060, primarily meeting demand growth rather than replacing coal generation. Nuclear remains relatively stable, accounting for 3%-6% of generation over 2021-2060. Storage deployment

https://doi.org/10.5194/egusphere-2026-1919
Preprint. Discussion started: 26 May 2026

remains limited, consistent with the low share of variable renewables. Overall, REF maintains a fossil-dominated generation mix with high emissions.

By contrast, the CN scenario shows a fundamental shift in the power system, driven by the rapid deployment of renewables. Solar expands from 4% in 2021 to 48% in 2060, becoming the largest source of generation. Wind also increases to 27% in 2060, with offshore deployment concentrated in coastal provinces. This expansion is accompanied by a decline of fossil generation: coal generation falls from 20 EJ to 2 EJ by 2060, with remaining capacity retrofitted with CCS, reaching 95% of coal generation by 2060. Gas generation declines to 1%, with remaining output equipped with CCS. Nuclear and hydropower remain relatively stable, together accounting for 17% of generation in 2060.

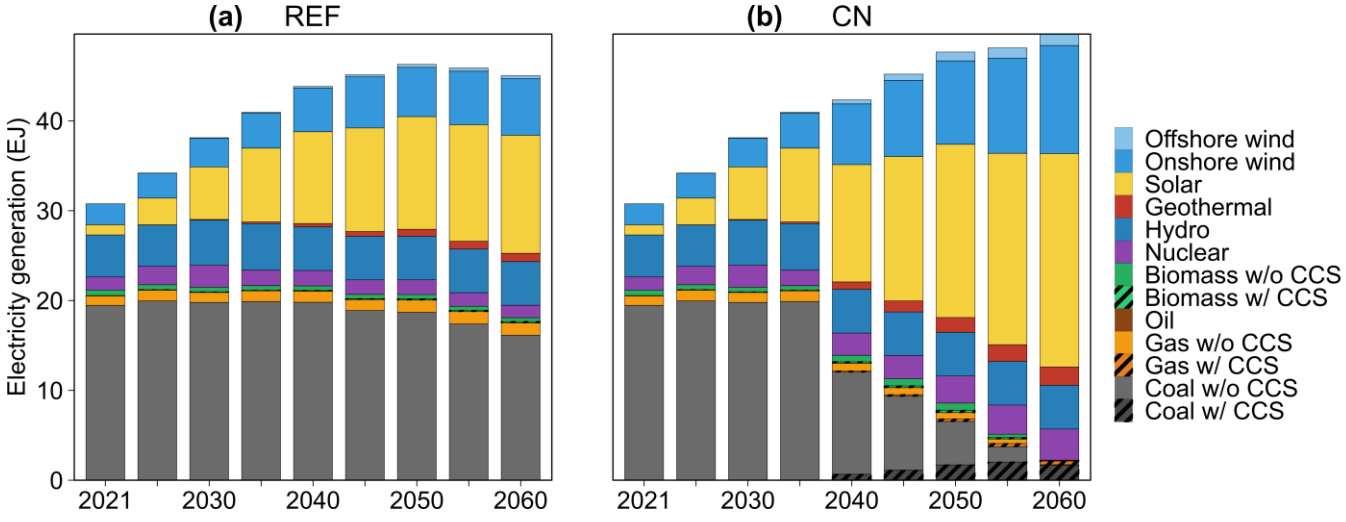

Figure 2: Electricity-generation mix for the reference and carbon-neutrality scenario.

(2) Regional distribution of electricity generation

Figure 3 shows provincial non-fossil generation shares in 2060 under the REF and CN scenarios. In CN, all provinces exceed 85%, with many reaching above 90%, indicating a near-complete phase-out of fossil generation. In REF, the distribution remains uneven: only parts of Southwest exceed 80%, while many provinces remain in the 42%-76% range.

Furthermore, a consistent regional pattern is observed in both scenarios. The Southwest has the highest non-fossil shares, reaching 69%-99% under REF, supported by hydropower and wind resources. The Northeast and North China remain more fossil-dependent, with shares of 47%-69% in 2060. Compared with REF, non-fossil shares in CN are higher by 20-40 percentage points across most provinces. CN produces a uniformly high non-fossil electric power system, while REF retains substantial regional variation.

https://doi.org/10.5194/egusphere-2026-1919
Preprint. Discussion started: 26 May 2026

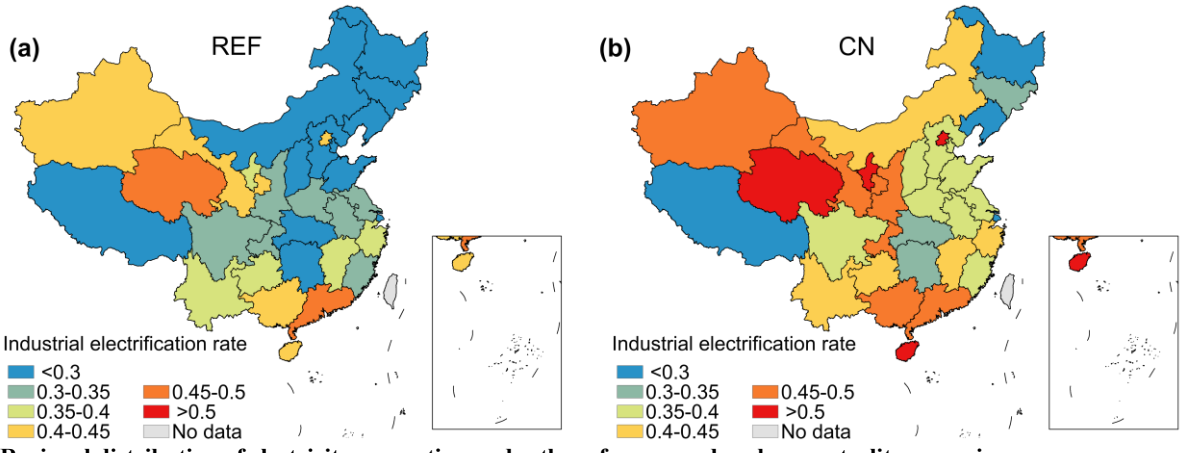

Figure 3: Regional distribution of electricity generation under the reference and carbon neutrality scenarios.

(3) Coal generation by vintage

Disaggregating coal-fired power generation by construction vintage reveals heterogeneity in the age structure of coal generation across provinces (Figure 4). In 2021, old vintages (pre-2010) accounted for 75% and 59% of total generation in Hebei and Jiangsu, respectively. By contrast, in Xinjiang and Anhui, where generation is dominated by units commissioned after 2010, older vintages contribute only 12% and 44% of total generation. These differences lead to distinct coal retirement trajectories across provinces.

Figure 4 shows results under the REF scenario. Coal generation from older vintages declines from 11 EJ in 2021 to 5 EJ in 2040, while newer vintages continue operating through mid-century. Compared with a non-vintage representation (black line), which retires all coal capacity at a similar rate, the vintage-based approach produces a staggered retirement pathway. In provinces with older fleets, such as Hebei and Jiangsu, coal generation declines by 14% and 9% by 2040. In contrast, provinces with newer capacity, such as Xinjiang and Anhui, experience slower declines of 14% and 8% over the same period. As a result, coal phase-out follows the existing age structure of capacity, with earlier retirements in eastern provinces and later retirements in western regions. Province abbreviations are provided in Supplementary Table SM5.

https://doi.org/10.5194/egusphere-2026-1919
Preprint. Discussion started: 26 May 2026

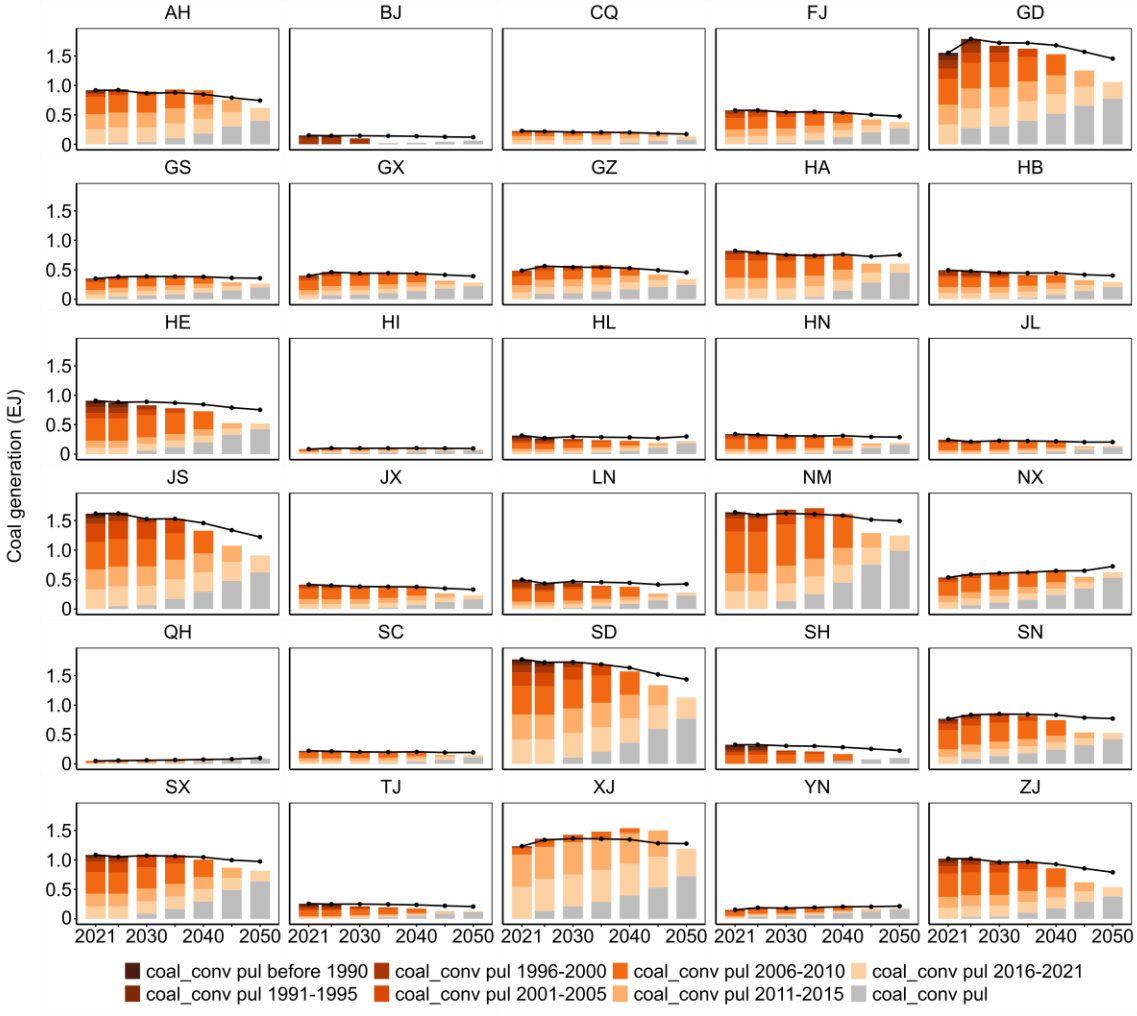

Figure 4: Coal-fired power generation by construction vintage across Chinese provinces under REF.

3.1.2 Industry

Figure 5 compares final energy use under the REF and CN scenarios. In REF, the energy mix remains dominated by fossil fuels, with coal accounting for 43% in 2021 and 34% in 2060, and only limited growth in electricity to 31%. In CN, direct coal declines to 19% by 2060, while electricity and hydrogen increase to 40% and 13%, respectively. Total final energy demand declines from 68 EJ to 64 EJ over 2021-2060, reflecting efficiency improvements and structural change. The transition also varies across subsectors, depending on production technologies and the relative importance of combustion versus process emissions.

https://doi.org/10.5194/egusphere-2026-1919
Preprint. Discussion started: 26 May 2026

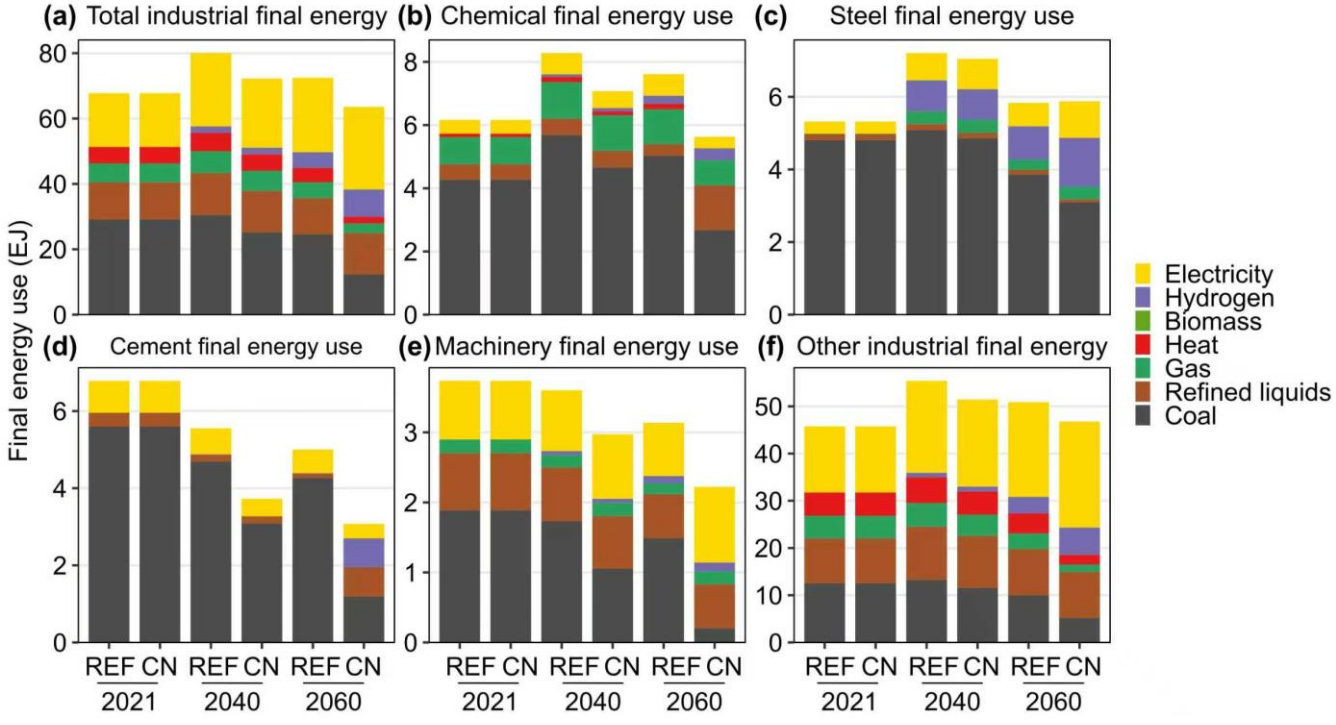

Figure 5: Final energy use in the industry sector under the REF and CN scenario.

The largest change occurs in energy-intensive materials in the CN scenario, as shown in Fig.6. In steel, the share of blast-furnace/basic-oxygen furnace (BF-BOF) production declines from 89% in 2021 to 64% in 2060, while scrap-based electric furnaces increase to 21%, and hydrogen-based direct reduced iron reaches 11%. Coal use in steel declines by 36%, with remaining emissions managed through CCS, which is applied to 30% of production by 2060. In cement, total output changes from 2 Gt to 0.8 Gt, while total final energy demand declines by 55%. Fossil fuel use decreases from 88% to 63%, and CCS deployment reaches 93% of clinker production, targeting process emissions from calcination. Across these sectors, emission reductions are achieved through a combination of fuel switching, electrification, and CCS deployment.

https://doi.org/10.5194/egusphere-2026-1919
Preprint. Discussion started: 26 May 2026

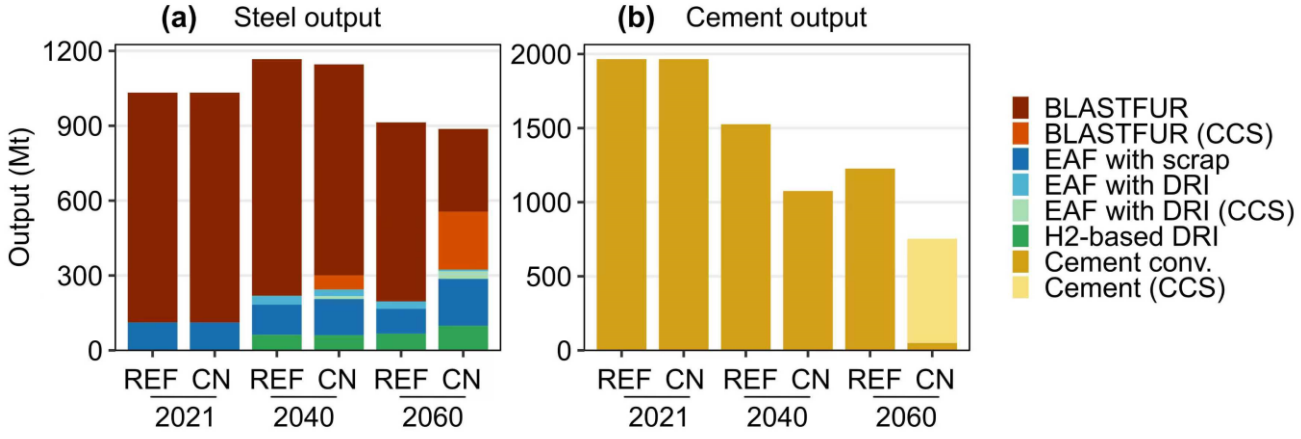

Figure 6: Production and technology transitions for the steel and cement sectors under the REF and CN scenario.

Process-intensive chemicals, machinery, and other industrial subsectors follow similar transition directions under the CN scenario, with differences in the balances between demand reduction and fuel substitution. In chemicals and N fertilizer, total final energy demand remains high, at nearly 6 EJ in 2060, with only slight changes in the energy mix. Fossil fuels decline marginally from 91% to 87% over 2021-2060, indicating continued dominance, while electricity and hydrogen increase to 7% and 13%, respectively. In machinery, final energy demand declines from 4 EJ to 2 EJ by 2060, representing a reduction of 41%, driven by rapid efficiency improvements and electrification. In "other industry", total activity remains relatively stable, while fossil fuel use declines from 42% to 35%, accompanied by an increase in electricity to 48%, indicating gradual electrification across diverse industrial applications.

Figure 7 shows the provincial distribution of industrial electrification. Under the REF scenario, electrification rates remain limited, with most provinces in the range of 18%-41% and only a few reaching 45%-50% by 2060. In contrast, the CN scenario shows a broad increase across provinces. Electrification rises to 24%-50% range in most regions, with several exceeding 50%. The national average electrification rate increases from 24% in 2021 to 40% in 2060, compared with 21%-31% under REF. Across regions, northwest and south provinces reach electrification levels of 30%-60%, while northeast and east provinces remain low at 24%-42%, reflecting differences in industrial structure and energy use.

https://doi.org/10.5194/egusphere-2026-1919
Preprint. Discussion started: 26 May 2026

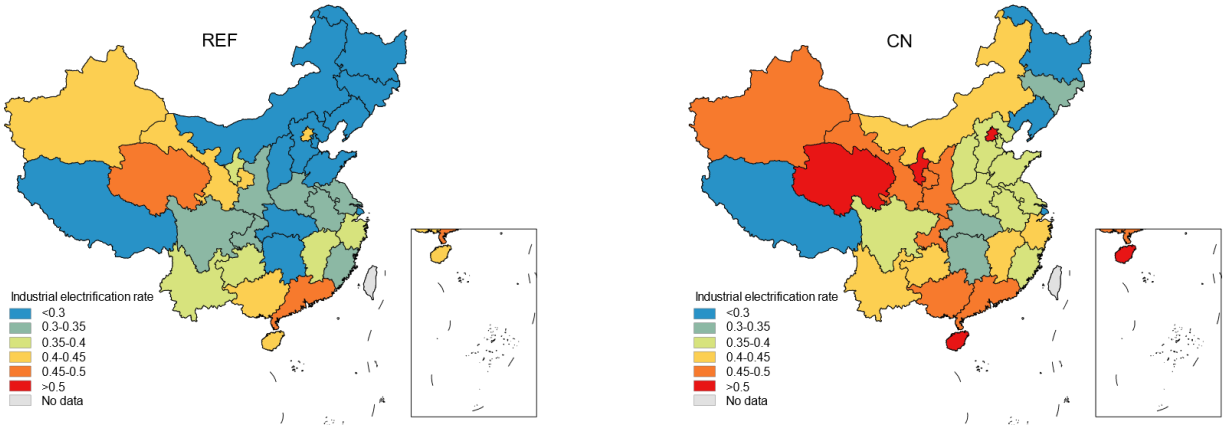

Figure 7: Spatial distribution of industrial electrification under the REF and CN scenario.

3.1.3 Buildings

The building sector shifts toward higher electrification and reduced use of solid fuels by 2060 (Fig.8). In the commercial sector, electricity increases from 4 EJ in 2021 to 9 EJ in REF and 10 EJ in CN by 2060, while LPG/NG and district heating decline correspondingly. The electrification rate surges from 70% in 2021 to 82% and 87% in the REF and CN, respectively. In urban residential buildings, electricity demand grows from 6 EJ in 2021 to 9 EJ by 2060, accounting for about 67% of the total service demand by 2060. Conversely, the share of LPG/NG declines from 25% to 20% and district heat from 15% to 13% under CN. Changes in REF are more limited. Service demand energy use in rural residential buildings peaks around 2030 and subsequently undergoes a steady decline due to urbanization. In 2021, coal and biomass demand were 0.8 EJ and 1.4 EJ, representing 12% and 19% of the energy mix, respectively. Over time, these traditional solid fuels undergo a phase-out. By 2060, coal decreases to 2% in REF and below 1% in CN, while electricity demand increases to roughly 4.8 EJ in REF and 5 EJ in CN, raising its share to 74% and 78%, respectively. Overall, electrification expands across all building types, with the most pronounced changes occurring in rural areas where solid fuels are largely replaced.

https://doi.org/10.5194/egusphere-2026-1919
Preprint. Discussion started: 26 May 2026

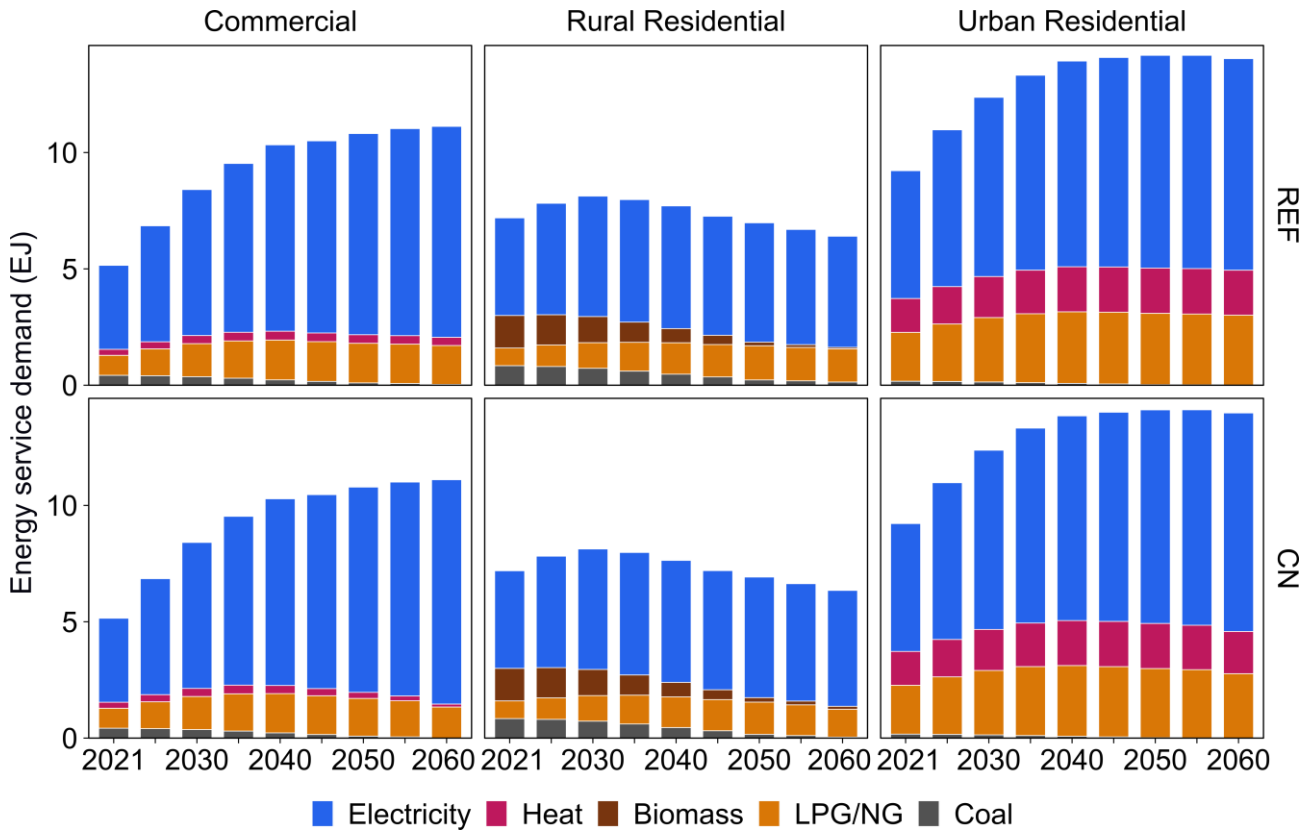

Figure 8: Energy service shares by fuel in the building sector.

3.1.4 Transportation

The transportation sector shifts from a petroleum-dominated system toward a diversified fuel mix in terms of service output (Fig.9). In the light-duty vehicle (LDV) sector, oil declines from 86% in 2021 to 58% in REF and 40% in CN by 2060 in service share. Electricity increases to 17% in REF and 35% in CN, while biomass liquids account for 15% in CN. In the heavy-duty vehicle (HDV) fleet, oil remains dominant in REF at 70% in 2060, with hydrogen and biomass liquids each contributing about 10% of service output. Under CN, oil declines to 56%, while hydrogen increases to 20%, and electricity and biomass liquids each reach about 13%. Compared with LDV, the transition in HDV relies more on fuel diversification rather than electrification alone.

https://doi.org/10.5194/egusphere-2026-1919
Preprint. Discussion started: 26 May 2026

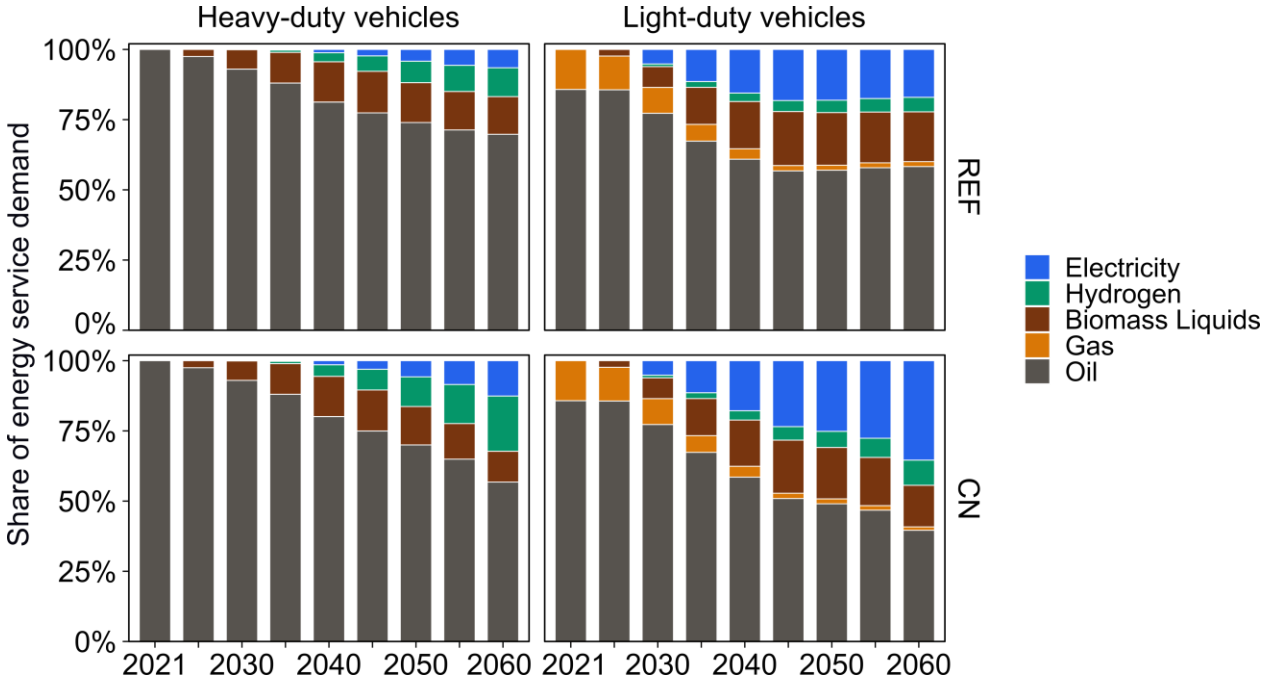

Figure 9: Energy service shares by fuel in light-duty and heavy-duty transport.

3.1.5 Resource

The updated resource supply curves show spatial variation in renewable energy potential and cost across China. At the national scale, the maximum potential of utility-scale solar PV is 359 EJ (Fig.10), compared with 139 EJ for onshore wind (Supplementary Figure SM1). Solar PV potential is concentrated in western and northern provinces, with Xinjiang (158 EJ) and Tibet (143 EJ) accounting for over 80% of the total, while eastern provinces such as Shanghai have minimal potential (0.1 EJ). Median LCOE for solar PV ranges from $0.0385/kWh in Sichuan to $0.0588/kWh in Chongqing, indicating relatively limited variation across provinces.

Onshore wind shows a similar spatial distribution. Inner Mongolia has the largest potential (52 EJ), followed by Xinjiang (29 EJ), while Chongqing (0.1 EJ) and Shanghai (0.1 EJ) have the smallest potential. Median LCOE ranges from $0.0142/kWh in Inner Mongolia to $0.0820/kWh in Chongqing, showing a wider cost range than solar PV. Resource-rich regions (e.g., Inner Mongolia) have lower costs, while provinces with limited resources have higher costs (e.g., Chongqing).

https://doi.org/10.5194/egusphere-2026-1919
Preprint. Discussion started: 26 May 2026

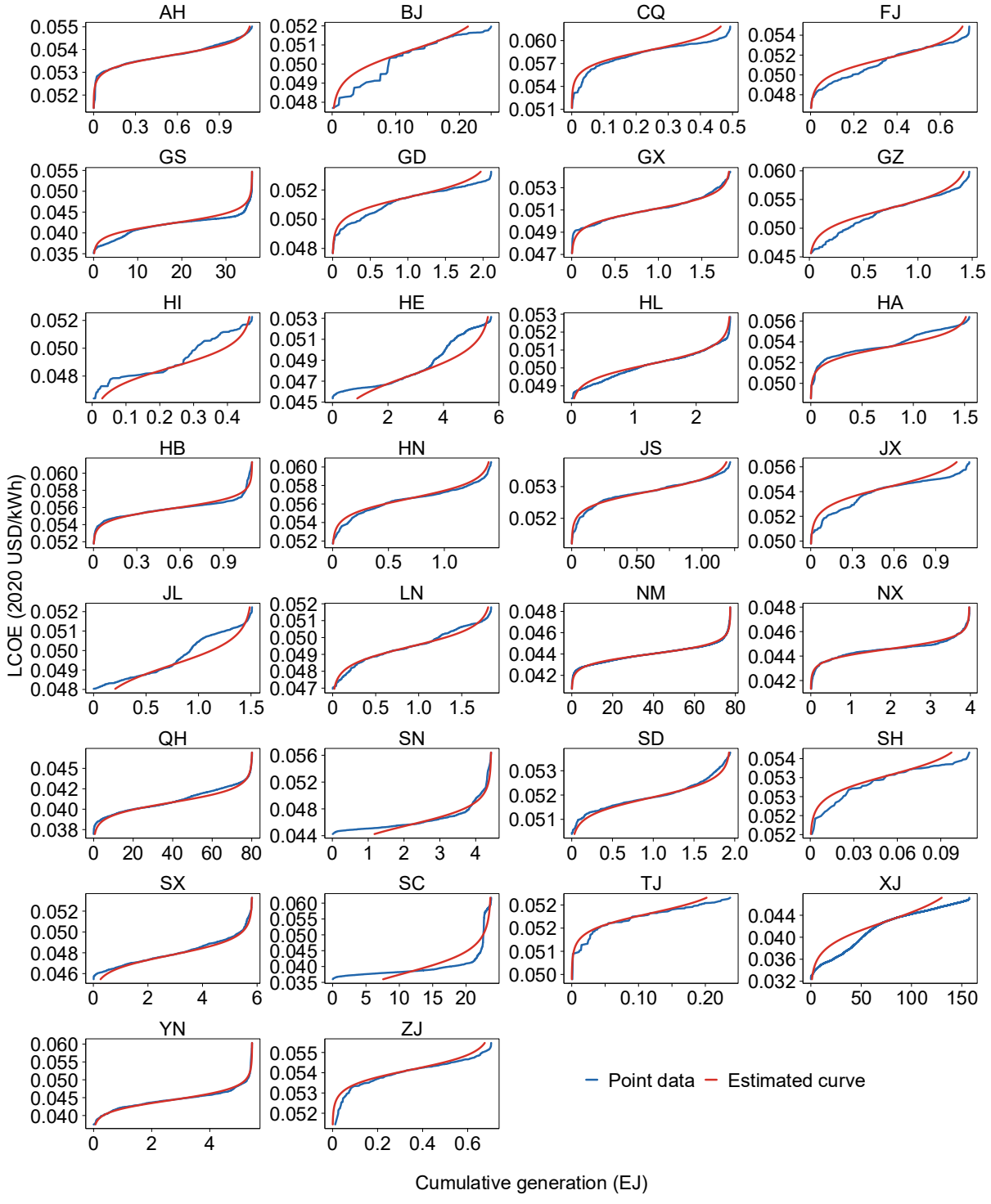

Figure 10: Resource supply curves for utility-scale solar PV.

https://doi.org/10.5194/egusphere-2026-1919
Preprint. Discussion started: 26 May 2026

3.1.6 Biomass

The model generates multiple variables for biomass resource exploitation, bioenergy production across different technologies, and both positive carbon emissions and negative carbon sequestration from bioenergy systems with CCS. Under the CN scenario, 9 EJ of residue resources will be utilized, and 8 EJ of purpose-grown energy crops will be cultivated on suitable land, covering approximately 363 thousand km^2 in 2060 (Fig.11). As for the carbon removal amount from BECCS, by 2030, BECCS remains in the nascent development stage, contributing zero net carbon removal to the energy and land system. By 2040, BECCS will have initial demand, though the scale will remain below 1MT CO_2. However, with the strengthening of China's climate policies and the mitigation demand from the hard-to-abate sector, BECCS will remove 0.3 $GtCO_2$ by 2050. By 2060, the total CDR amount from BECCS will reach 1 $GtCO_2$, accounting for 35% of the total CDR amount. At the provincial level, Jilin, Anhui, and Henan will lead the development of BECCS, removing 0.1, 0.07, and 0.06 $MtCO_2$ by BECCS in 2040. In 2060, Jilin and Anhui will remove 176 and 113 $MtCO_2$, contributing 16% and 10% of the removal amounts achieved by BECCS.

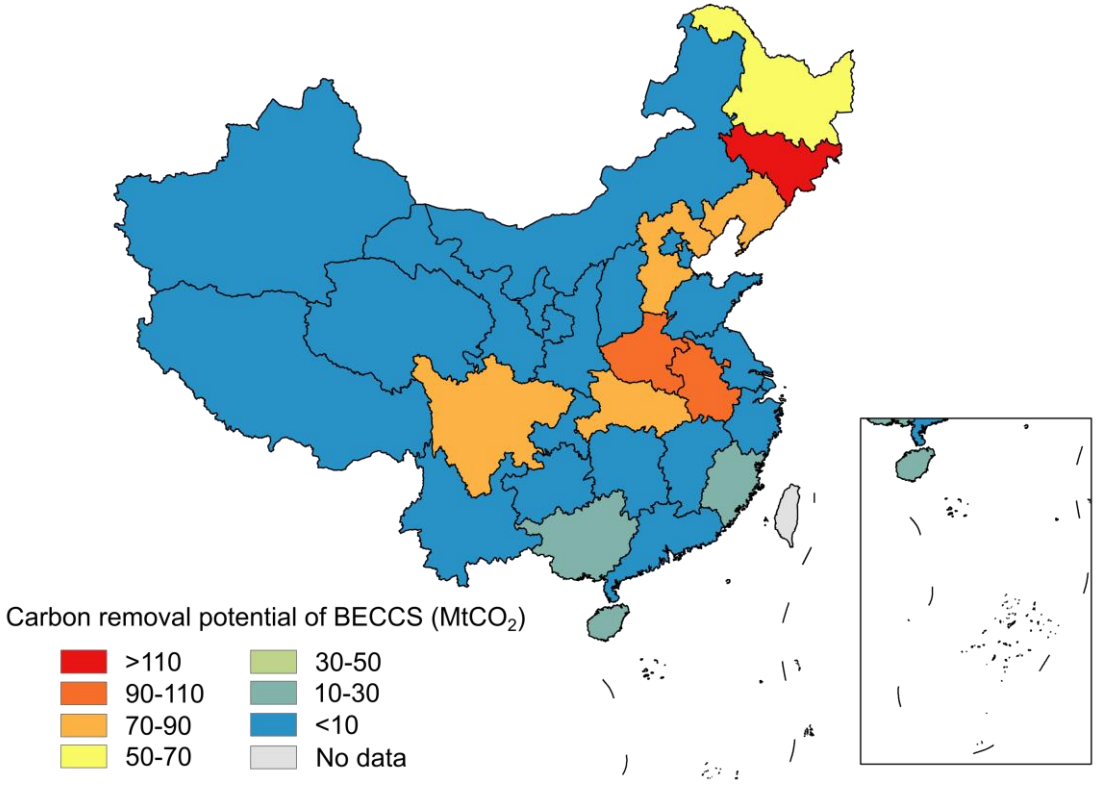

Figure 11: Spatial distribution of BECCS carbon removal across provinces in 2060 under CN.

https://doi.org/10.5194/egusphere-2026-1919
Preprint. Discussion started: 26 May 2026

3.2 Non-CO_2 greenhouse gas emissions

Compared with REF, the CN scenario shows stronger reductions in non-CO_2 greenhouse gas emissions (Fig.12). Aggregate CH_4 emissions in CN remain around 1,010 Mt CO_2-eq (using 100-year AR4 GWP) through 2030 and decline to 386 Mt CO_2-eq by 2060, compared with 756 Mt CO_2-eq in REF. N_2O emissions under CN decrease from 416Mt to 386 Mt CO_2-eq over 2021–2060, while remaining nearly constant in REF, resulting in a difference of about 7% in 2060. Emissions from energy use also decline under CN. CH_4 decreases from 31 Mt CO_2-eq in 2021 to 21 Mt CO_2-eq in 2060, compared with 26 Mt CO_2-eq in REF, while N_2O decreases to 22 Mt CO_2-eq under CN versus 28 Mt CO_2-eq in REF.

https://doi.org/10.5194/egusphere-2026-1919
Preprint. Discussion started: 26 May 2026

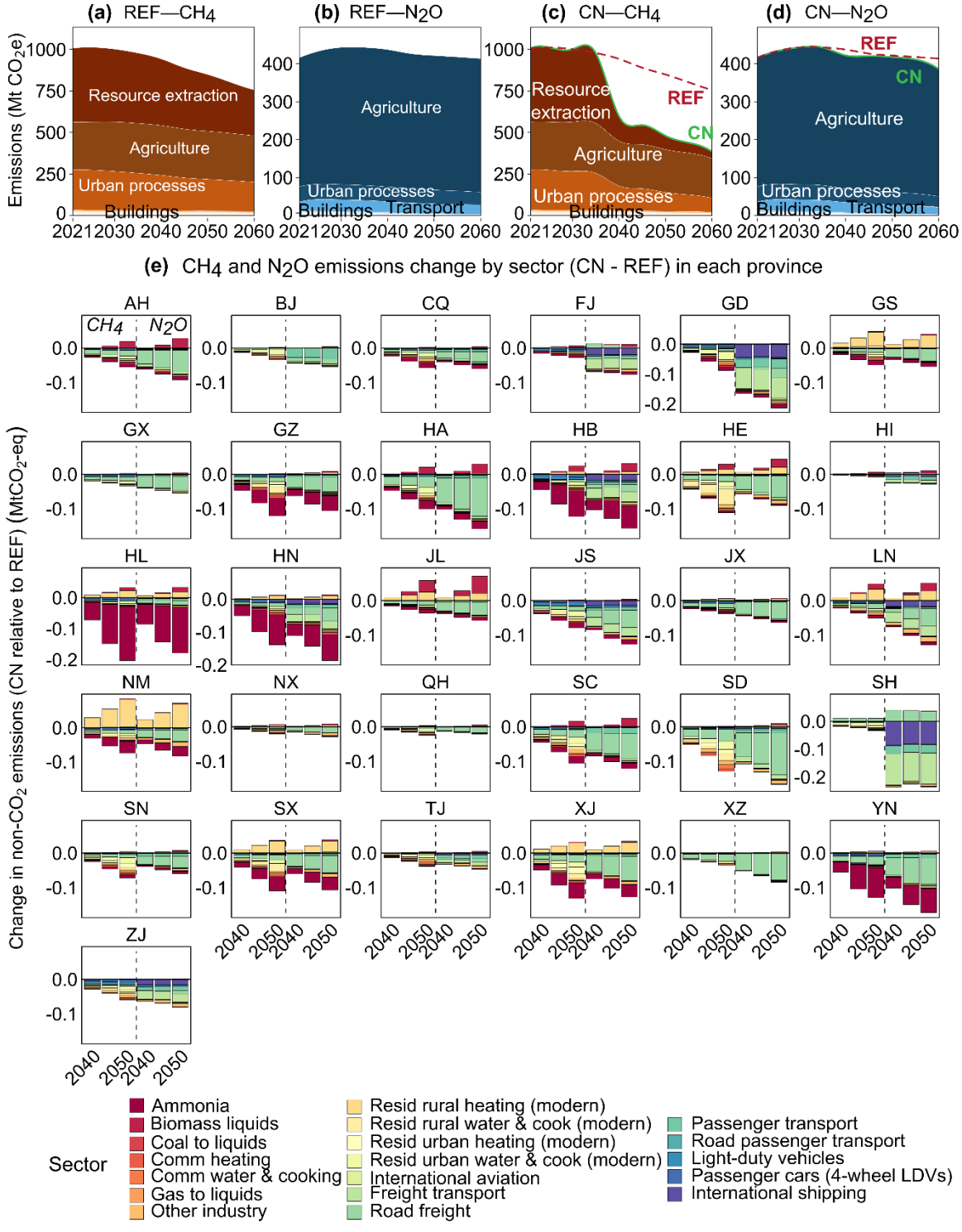

Figure 12: National and provincial non-CO_2 emissions from China's energy system under the REF and CN scenarios.

https://doi.org/10.5194/egusphere-2026-1919
Preprint. Discussion started: 26 May 2026

At the national level, as shown in Figure 12(a)-(d), the largest reduction in non-CO_2 emissions occurs in fossil resource extraction. Under CN, CH_4 emissions from coal mining decline from 376 Mt CO_2-eq in 2021 to 23 Mt CO_2-eq in 2060, almost 90% lower than REF in 2060. Additional reductions occur in energy end-use sectors. In ammonia production, CH4 emissions decrease by about 87%, from 1 to 0.2 Mt CO_2-eq over 2021-2060, while N_2O emissions decline from 2 to 0.02 Mt CO_2-eq. At the same time, some sources increase during the transition. N_2O emissions from biomass liquids increase from 0.004 Mt CO_2-eq in 2021 to 1 Mt CO_2-eq in 2060. These results show a shift in non-CO_2 emissions from fossil-based sources toward bioenergy sources under CN.

Spatially, the CN scenario shows substantial interprovincial variation in energy end-use non-CO_2 emissions (Figure 12(e)). In 2021, provincial CH_4 and N_2O emissions from energy end use ranged from about 0.3 Mt CO_2-eq in Hainan to roughly 5 Mt CO_2-eq in Hebei. By 2060, emissions decline in all provinces but remain uneven, spanning 0.2-3 Mt CO_2-eq. In provinces with low emissions, buildings account for a large share. For example, in Beijing, total emissions are 0.8 Mt CO_2-eq in 2021, with buildings accounting for 0.4 Mt CO_2-eq (53%), increasing to 57% by 2060. In contrast, provinces with higher emissions show a stronger contribution from transport and industry. In Anhui, total emissions reach 2 Mt CO_2-eq, more than twice that of Beijing, with buildings contributing about 25%. Road freight contributes about 1 Mt CO_2-eq in both 2021 and 2060, while emissions from biomass liquids grow from near zero in 2021 to 0.2 Mt CO_2-eq by 2060. Industrial process sources such as ammonia remain at 0.04 Mt CO_2-eq in 2021 and decline toward zero by mid-century.

3.3 Water use

Water use evolves differently for withdrawals and consumption over time (Fig.13). Total withdrawals follow a declining trend after mid-century, whereas total water consumption shows a more stable trajectory, varying within 210-235 km^3 over the projection period with only small differences between scenarios. Compared with REF, the CN mainly alters the sectoral composition of water use rather than total levels.

Water withdrawals follow an inverted-U pattern in both scenarios, increasing from 398 km^3 in 2021 to a peak of 432-433 km^3 around 2030-2040, and then declining to 395 km^3 in REF and 373 km^3 in CN by 2060. Irrigation remains the largest component, accounting for 35-40% of total withdrawals throughout. The post-peak decline is mainly driven by electricity generation, with withdrawals decreasing from 69 km^3 to 52 km^3 by 2060. Manufacturing and municipal withdrawals increase from 164 to 188 km^3 in early periods and then stabilize, while livestock and primary energy remain below 7% of the national total withdrawals. Compared with REF, electricity-related withdrawals decline earlier and more strongly under CN, resulting in a difference of 23 km^3 in total withdrawals by 2060. In contrast, irrigation withdrawals remain similar across scenarios.

Water consumption follows a different pattern from withdrawals. Total consumption increases from 210 km^3 in 2021 to 230 km^3 by 2030 and then stabilizes at 223-235 km^3 through 2060, with similar values in both scenarios. Irrigation remains the

https://doi.org/10.5194/egusphere-2026-1919
Preprint. Discussion started: 26 May 2026

dominant component, accounting for 35-38% of total consumption, followed by manufacturing and municipal uses at 23% and 17%, respectively. Electricity generation contributes about 14-17% and remains relatively stable after mid-century, while livestock increases slightly from 17 to 20 km^3, and primary energy remains negligible. Differences between REF and CN are small, with total consumption differing by less than 2% in 2060.

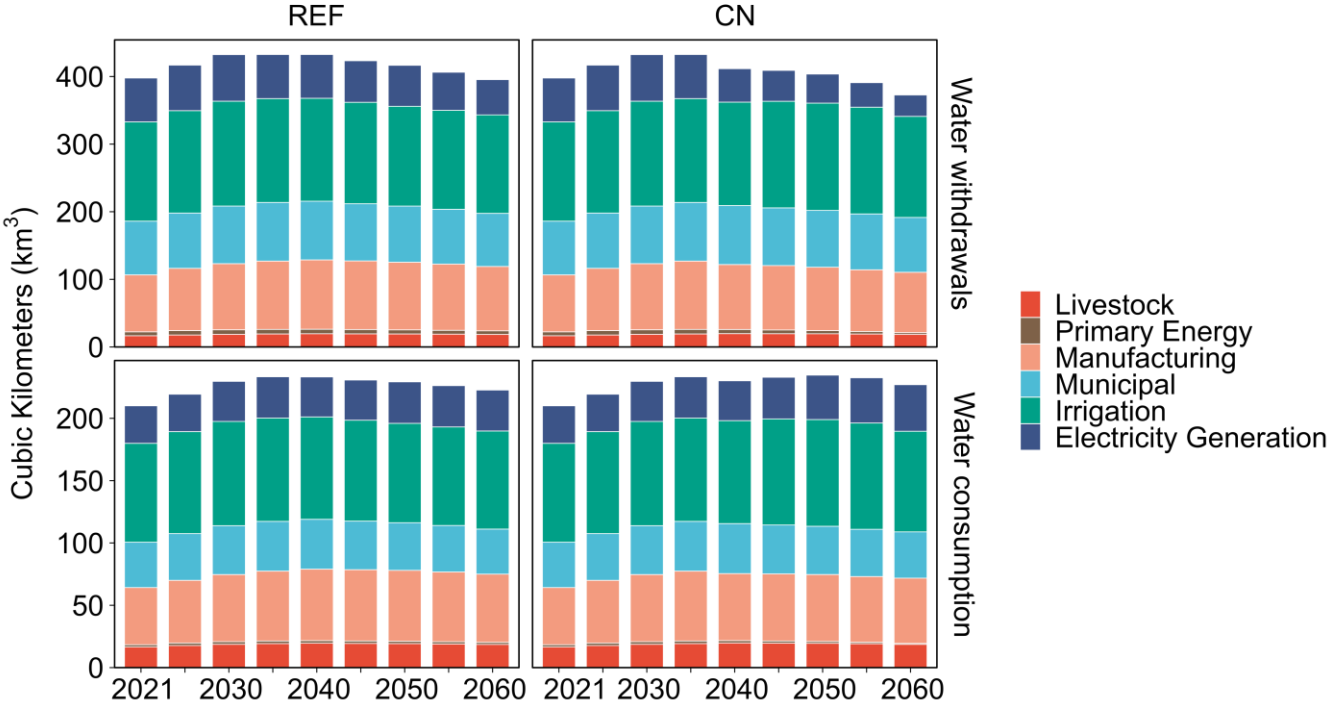

Figure 13: Water withdrawals and consumption by sector under REF and CN scenarios.

3.4 Example of an incentive policy for nuclear electricity generation

Policy-induced changes in nuclear electricity generation are shown in Fig.14. In addition to the REF and CN scenarios, two policy variants (REF-with-policy and CN-with-policy) are introduced to demonstrate provincial incentives for nuclear-based-load electricity generation. The four GCAM-China-v8 scenarios exhibit significantly different future trends of nuclear electricity generation (Figure 14a). In 2021, Guangdong had the largest nuclear generation at 0.4 EJ, followed by Fujian (0.3 EJ), Zhejiang (0.3 EJ), and Shandong (0.1 EJ). Policy incentives increase electricity generation from Generation II nuclear technology (nuc_base_Gen II) in all four provinces. Under CN-with-policy, generation from nuc_base_Gen II increases by 0.2 EJ in Fujian, 0.4 EJ in Guangdong, 0.1 EJ in Shandong, and 0.2 EJ in Zhejiang in 2060 relative to CN, reflecting the effect of our designed policy-induced changes.

Despite the policy implementation from 2021 to 2060, increases in electricity generation from Generation II nuclear technology decline after 2040 in both REF-with-policy and CN-with-policy scenarios (Figure 14b). In contrast to the overall

https://doi.org/10.5194/egusphere-2026-1919
Preprint. Discussion started: 26 May 2026

increase in nuc_base_Gen II, changes in electricity generation from nuc_base_Gen III are smaller and even negative across provinces, particularly under CN. Overall, policy effects similarly increase nuc_base_Gen II under both CN and REF scenarios, while compressing nuc_base_Gen III deployment more significantly under CN.

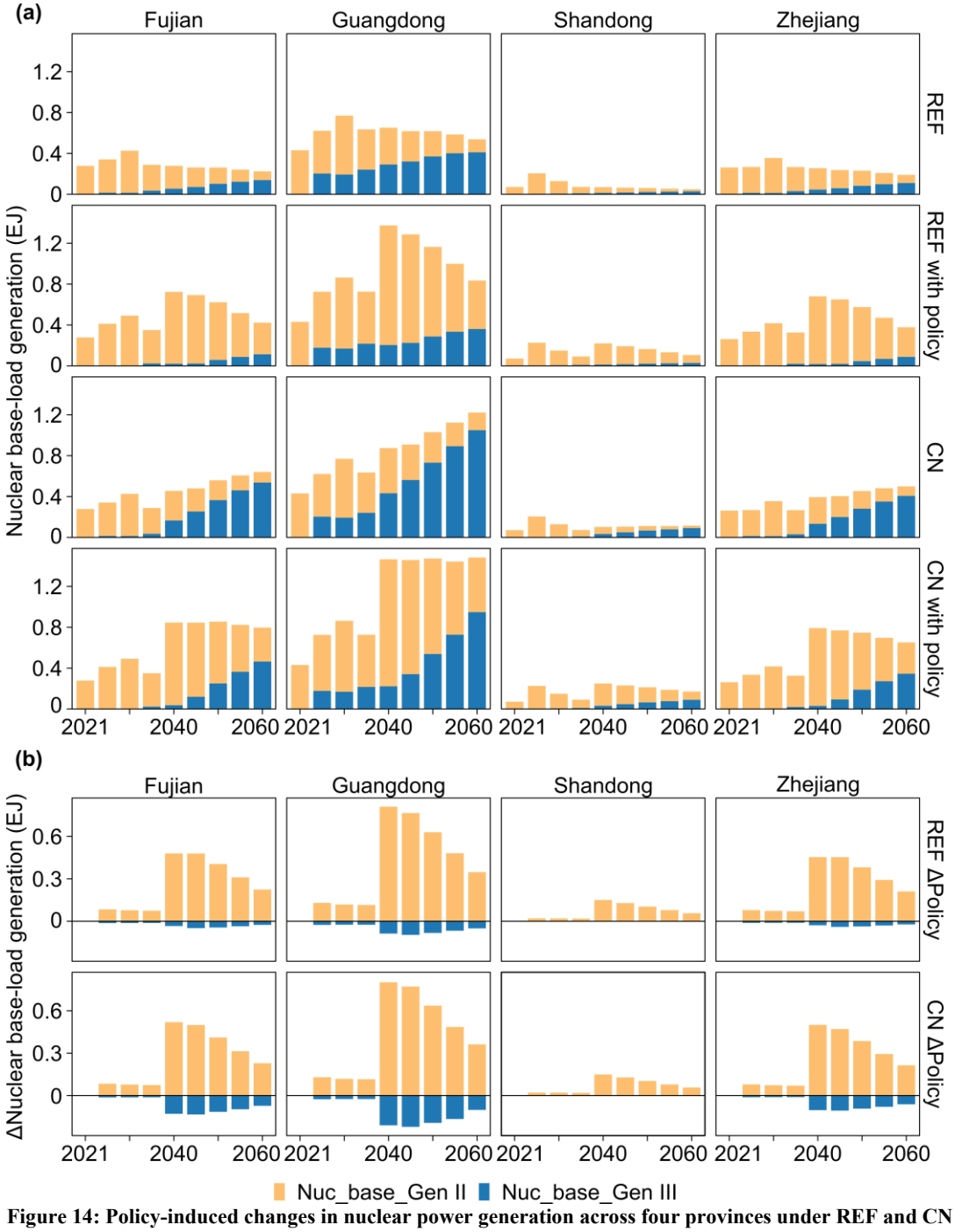

Figure 14: Policy-induced changes in nuclear power generation across four provinces under REF and CN scenarios (2021-2060).

https://doi.org/10.5194/egusphere-2026-1919
Preprint. Discussion started: 26 May 2026

3.5 Comparison to historical data

GCAM-China-v8 aligns with historical provincial energy CO_2 emissions and electricity generation with reasonable agreement across historical calibration years (2005, 2010, 2015, and 2021). Provincial energy-system CO_2 emissions are compared with the MEIC database (Zheng et al., 2018), and electricity generation with data from China Electricity Council (2021). Model performance is assessed using one-to-one comparisons between historical values (x-axis) and GCAM-China-v8 REF values (y-axis) at the provincial level, together with a 1:1 line and a ±5% deviation band (Fig.15 (a)-(d) for CO_2 and Fig.15 (e)-(h) for electricity).

For provincial energy CO_2, model values are generally distributed along the 1:1 line. The number of provinces within ±10% of historical values is 16 (2005), 20 (2010), 20 (2015), and 18 (2021), while the number within ±5% is 10, 14, 14, and 11, respectively. For provincial electricity generation, agreement is generally higher. The number of provinces within ±10% is 25 (2005), 12 (2010), 28 (2015), and 25 (2021), and the number within ±5% is 21, 5, 24, and 22, respectively. Provincial values cluster closely around the 1:1 line across all years. Overall, GCAM-China-v8 reproduces the provincial distribution and magnitude of both energy CO_2 emissions and electricity generation over historical periods.

https://doi.org/10.5194/egusphere-2026-1919
Preprint. Discussion started: 26 May 2026

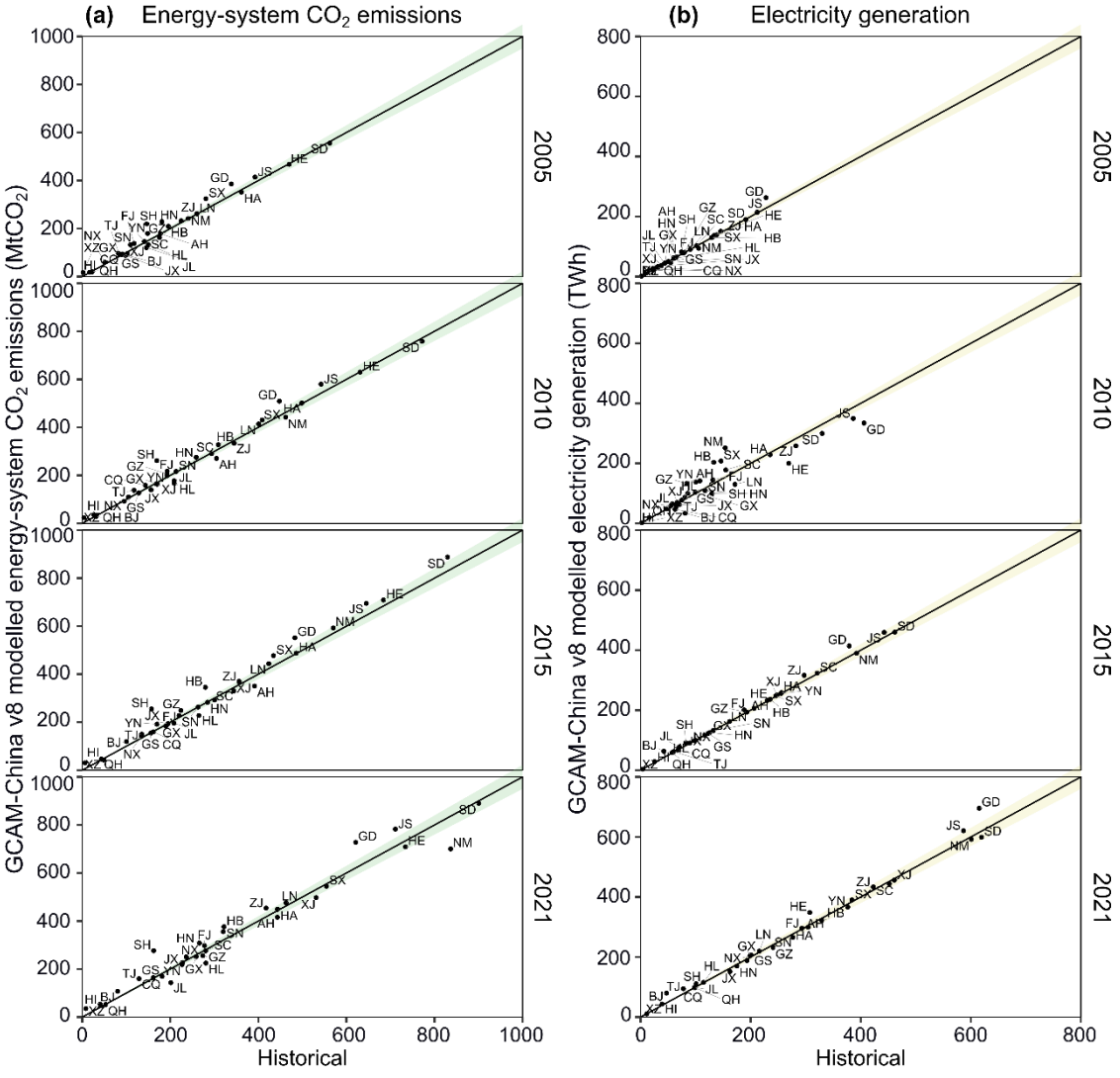

Figure 15: **GCAM-China-v8 results versus historical inventory data.**

4 Discussion and conclusions

This study provides a comprehensive methodological documentation of GCAM-China-v8. As the first dedicated documentation of the GCAM-China, this study demonstrates the model's capability to represent subnational heterogeneity in energy, emissions, and resource systems. By incorporating provincial-level differences in resource endowments, socioeconomic drivers, and sectoral structures, GCAM-China-v8 enables a more detailed assessment of China's transition pathways at the provincial scale. Its integration within the global GCAM framework further allows for consistent analysis of interactions between China and the rest of the world.

https://doi.org/10.5194/egusphere-2026-1919
Preprint. Discussion started: 26 May 2026

This study demonstrates several key system-wide features of China's low-carbon transition. Electrification plays a central role across end-use sectors, while non-CO_2 emissions exhibit uneven mitigation patterns across sectors and regions. Water demand shows a clear divergence between withdrawals and consumption, with reductions in carbon neutrality primarily driven by changes in the power sector. In addition, biomass deployment and BECCS exhibit strong spatial concentration, indicating potential regional constraints on negative emissions. Like many national analyses in the US (Shi et al., 2017), Canada (Younis et al., 2025b), and Korea (Jeon et al., 2021b), our results emphasize the importance of representing subnational heterogeneity in integrated assessment modeling.

Despite these advances, several limitations remain. First, the power sector operates on an annual balance and does not include sub-annual temporal resolution, limiting the representation of variability in electricity demand and its influence on long-term capacity planning (Ou et al., 2021c). Second, inter-provincial electricity trade is represented in a simplified manner and does not explicitly capture transmission constraints or grid topology. Third, the transportation sector largely follows the aggregated structure of the GCAM framework and lacks detailed representations of China's transportation modes and technology structure (Shao et al., 2024). Finally, policy representation remains limited, with one nuclear expansion example for demonstration. Future work will develop a full policy module to better reflect the complex policy architecture in China.

Future development of GCAM-China will extend beyond incremental GCAM model refinements to better capture the unique features of China's energy transition. For example, representing the emerging "new energy system" will require explicit treatment of integrated source-grid-load-storage interactions (Dowling et al., 2020), including the coordination of variable renewable generation (Tong et al., 2021), grid flexibility (Davis et al., 2018), and power system security (Li et al., 2025). In parallel, electricity demand from data center and digital infrastructure is increasing rapidly in China and worldwide (Zhang, 2026), which needs to be explicitly represented in the model.

In addition, further advances will require expanding the representation of socioeconomic dynamics that are particularly relevant in China. This includes incorporating heterogeneous and dynamic consumer behavior (McCollum et al., 2017), income-driven demand evolution (Wolfram et al., 2012), and policy-driven diffusion of low-carbon technologies at the subnational level (Mi and Sun, 2021). These extensions are constrained by limited empirical evidence for key processes (Selin et al., 2023), particularly the parameterization and validation of consumer behavior, technology adoption, and emerging energy services at the provincial level. Despite these challenges, the development of GCAM-China-v8 and this documentation provide a useful case for representing subnational heterogeneity and offer a reference for extending integrated assessment models to other countries.

https://doi.org/10.5194/egusphere-2026-1919
Preprint. Discussion started: 26 May 2026

Code and data availability

GCAM-China is an open-source model available at: https://doi.org/10.5281/zenodo.19471594 (Center for Global Sustainability at University of Maryland et al., 2026). The processing code and scenario data of this study will be publicly available upon publication.

Author contributions

SX and YO led the writing of the paper and model development with contributions from YL, SY, WD, YJ, YQL, ZL, JXS, JYS, CW (BIT), HW, RW, FW, HZ, MZ, and RZ; Preliminary data collection and model development were conducted by JB, MB, JC, RD, CD, SD, JF, MG, CG, JH, HK, CL, BL, AM, XP, PP, MQ, YQ, TS, YS, LW, YY, BY, ZY, JZ, QZZ; WJC, WYC, LC, RC, NH, BGL, JL, XL, HM, BW, CW (TU), PW, SW, ZW, LZ, and QZ contributed to project supervision.

Competing interests

The authors declare that they have no conflict of interest.

Acknowledgements

MB, JF, MG, PP, YQ, and BY are employed by Pacific Northwest National Laboratory, but no U.S. government funding was used to support this work. The authors gratefully acknowledge Jeff McLeod for his contributions to the early-stage development of GCAM-China.

Financial support

This work is supported by the National Natural Science Foundation of China (grant no. 72474002; 72534005; 42305190; L2524074; 52225902); the National Key R&D Program of China (grant no. 2024YFF1307000; 2023YFC3708500); Bloomberg Philanthropies. SY, RC, NH, AM, JB, and CG are supported by Sequoia Climate Foundation. JF and HK are supported by ClimateWorks Foundation.

References

Asia-Pacific Economic Cooperation (APEC): Ethanol and biodiesel production data, 2015.

Bosetti, V. and Longden, T.: Light duty vehicle transportation and global climate policy: The importance of electric drive vehicles, Energy Policy, 58, 209–219, https://doi.org/10.1016/j.enpol.2013.03.008, 2013.

https://doi.org/10.5194/egusphere-2026-1919
Preprint. Discussion started: 26 May 2026

Calvin, K., Wise, M., Kyle, P., Patel, P., Clarke, L., and Edmonds, J.: Trade-offs of different land and bioenergy policies on the path to achieving climate targets, Clim. Change, 123, 691–704, https://doi.org/10.1007/s10584-013-0897-y, 2014.

Calvin, K., Bond-Lamberty, B., Clarke, L., Edmonds, J., Eom, J., Hartin, C., Kim, S., Kyle, P., Link, R., Moss, R., McJeon, H., Patel, P., Smith, S., Waldhoff, S., and Wise, M.: The SSP4: A world of deepening inequality, Glob. Environ. Change, 42, 284–296, https://doi.org/10.1016/j.gloenvcha.2016.06.010, 2017.

Calvin, K., Patel, P., Clarke, L., Asrar, G., Bond-Lamberty, B., Cui, R. Y., Di Vittorio, A., Dorheim, K., Edmonds, J., Hartin, C., Hejazi, M., Horowitz, R., Iyer, G., Kyle, P., Kim, S., Link, R., McJeon, H., Smith, S. J., Snyder, A., Waldhoff, S., and Wise, M.: GCAM v5.1: representing the linkages between energy, water, land, climate, and economic systems, Geosci. Model Dev., 12, 677–698, https://doi.org/10.5194/gmd-12-677-2019, 2019.

Casper, K. C., Narayan, K. B., O'Neill, B. C., Waldhoff, S. T., Zhang, Y., and Wejnert-Depue, C. P.: Non-parametric projections of the net-income distribution for all U.S. states for the Shared Socioeconomic Pathways, Environ. Res. Lett., 18, 114001, https://doi.org/10.1088/1748-9326/acf9b8, 2023.

Center for Global Sustainability at University of Maryland, Department of Earth System Science at Tsinghua University, and College of Environmental Sciences Engineering at Peking University: umd-cgs/gcam-china: gcam-china-v8, https://doi.org/10.5281/zenodo.19471594, 2026.

Chaturvedi, V. and Kim, S. H.: Long term energy and emission implications of a global shift to electricity-based public rail transportation system, Energy Policy, 81, 176–185, https://doi.org/10.1016/j.enpol.2014.11.013, 2015.

Chen, S., Xiao, Y., Zhang, C., Lu, X., He, K., and Hao, J.: Cost dynamics of onshore wind energy in the context of China's carbon neutrality target, Environ. Sci. Ecotechnology, 19, 100323, https://doi.org/10.1016/j.ese.2023.100323, 2024.

Chen, Y., Guo, F., Wang, J., Cai, W., Wang, C., and Wang, K.: Provincial and gridded population projection for China under shared socioeconomic pathways from 2010 to 2100, Sci. Data, 7, 83, https://doi.org/10.1038/s41597-020-0421-y, 2020.

Cheng, J., Tong, D., Zhang, Q., Liu, Y., Lei, Y., Yan, G., Yan, L., Yu, S., Cui, R. Y., Clarke, L., Geng, G., Zheng, B., Zhang, X., Davis, S. J., and He, K.: Pathways of China's PM2.5 air quality 2015–2060 in the context of carbon neutrality, Natl. Sci. Rev., 8, nwab078, https://doi.org/10.1093/nsr/nwab078, 2021a.

Cheng, J., Tong, D., Zhang, Q., Liu, Y., Lei, Y., Yan, G., Yan, L., Yu, S., Cui, R. Y., Clarke, L., Geng, G., Zheng, B., Zhang, X., Davis, S. J., and He, K.: Pathways of China's PM2.5 air quality 2015–2060 in the context of carbon neutrality, Natl. Sci. Rev., 8, nwab078, https://doi.org/10.1093/nsr/nwab078, 2021b.

Cheng, J., Tong, D., Liu, Y., Geng, G., Davis, S. J., He, K., and Zhang, Q.: A synergistic approach to air pollution control and carbon neutrality in China can avoid millions of premature deaths annually by 2060, One Earth, 6, 978–989, https://doi.org/10.1016/j.oneear.2023.07.007, 2023.

China Electricity Council: Compilation of Statistical Data for Electric Power Industry, 2005.

China Electricity Council: China Electric Power Statistical Yearbook, 2021.

China Nuclear Energy Association: The China Nuclear Energy Development Report, 2025.

Chini, C. M., Djehdian, L. A., Lubega, W. N., and Stillwell, A. S.: Virtual water transfers of the US electric grid, Nat. Energy, 3, 1115–1123, https://doi.org/10.1038/s41560-018-0266-1, 2018.

https://doi.org/10.5194/egusphere-2026-1919
Preprint. Discussion started: 26 May 2026

Clarke, J. F. and Edmonds, J. A.: Modelling energy technologies in a competitive market, Energy Econ., 15, 123–129, https://doi.org/10.1016/0140-9883(93)90031-L, 1993a.

Clarke, J. F. and Edmonds, J. A.: Modelling energy technologies in a competitive market, Energy Econ., 15, 123–129, https://doi.org/10.1016/0140-9883(93)90031-L, 1993b.

Clarke, L., Jiang, K., Akimoto, K., Babiker, M., Fisher-Vanden, K., Hourcade, J.-C., Krey, V., Löschel, A., McCollum, D., Paltsev, S., Rose, S., Shukla, P. R., Tavoni, M., van, B., Böttcher, H., Calvin, K., Daenzer, K., Chen, W., Weyant, J., and Sokka, L.: Assessing Transformation Pathways, 2014.

Cui, R. Y., Hultman, N., Cui, D., McJeon, H., Yu, S., Edwards, M. R., Sen, A., Song, K., Bowman, C., Clarke, L., Kang, J., Lou, J., Yang, F., Yuan, J., Zhang, W., and Zhu, M.: A plant-by-plant strategy for high-ambition coal power phaseout in China, Nat. Commun., 12, 1468, https://doi.org/10.1038/s41467-021-21786-0, 2021a.

Cui, R. Y., Hultman, N., Cui, D., McJeon, H., Yu, S., Edwards, M. R., Sen, A., Song, K., Bowman, C., Clarke, L., Kang, J., Lou, J., Yang, F., Yuan, J., Zhang, W., and Zhu, M.: A plant-by-plant strategy for high-ambition coal power phaseout in China, Nat. Commun., 12, 1468, https://doi.org/10.1038/s41467-021-21786-0, 2021b.

Dahowski, R. T., Davidson, C. L., Yu, S., Horing, J. D., Wei, N., Clarke, L. E., and Bender, S. R.: The Impact of CCS Readiness on the Evolution of China's Electric Power Sector, Energy Procedia, 114, 6631–6637, https://doi.org/10.1016/j.egypro.2017.03.1817, 2017.

Das, P., Chaturvedi, V., Rajbanshi, J., Khan, Z. A., Kumar, S., and Goenka, A.: A new scenario set for informing pathways to India's next nationally determined contribution and 2070 net-zero target: structural reforms, LIFE, and sectoral pathways, Energy Clim. Change, 6, 100192, https://doi.org/10.1016/j.egycc.2025.100192, 2025.

Davis, S. J., Lewis, N. S., Shaner, M., Aggarwal, S., Arent, D., Azevedo, I. L., Benson, S. M., Bradley, T., Brouwer, J., Chiang, Y.-M., Clack, C. T. M., Cohen, A., Doig, S., Edmonds, J., Fennell, P., Field, C. B., Hannegan, B., Hodge, B.-M., Hoffert, M. I., Ingersoll, E., Jaramillo, P., Lackner, K. S., Mach, K. J., Mastrandrea, M., Ogden, J., Peterson, P. F., Sanchez, D. L., Sperling, D., Stagner, J., Trancik, J. E., Yang, C.-J., and Caldeira, K.: Net-zero emissions energy systems, Science, 360, eaas9793, https://doi.org/10.1126/science.aas9793, 2018.

Deng, S., Mi, Z., Ou, Y., Xu, H., Wei, S., Zhao, Y., Zhang, H., Qin, Z., and Piao, S.: Sustainability nexus in China's forestation initiatives, Nexus, 2, https://doi.org/10.1016/j.ynexs.2025.100106, 2025.

Diachuk, O., Kholod, N., Podolets, R., Graham, N., Semeniuk, A., Evans, M., Westphal, M. I., Stelmach, T., Hoesly, R., Trypolska, G., and Zagoruichyk, A.: Pathways for decarbonization of the buildings sector in Ukraine, Energy Clim. Change, 6, 100195, https://doi.org/10.1016/j.egycc.2025.100195, 2025.

Dong, J., Li, S., Sun, Y., Gong, W., Song, G., Ding, Y., Yang, J., Teng, M., Wang, R., Xing, J., Ou, Y., and Gong, W.: Provincial equity and enhanced health are key drivers for China's 2060 carbon neutrality, J. Clean. Prod., 473, 143531, https://doi.org/10.1016/j.jclepro.2024.143531, 2024.

Dowling, J. A., Rinaldi, K. Z., Ruggles, T. H., Davis, S. J., Yuan, M., Tong, F., Lewis, N. S., and Caldeira, K.: Role of Long-Duration Energy Storage in Variable Renewable Electricity Systems, Joule, 4, 1907–1928, https://doi.org/10.1016/j.joule.2020.07.007, 2020.

Eurek, K., Sullivan, P., Gleason, M., Hettinger, D., Heimiller, D., and Lopez, A.: An improved global wind resource estimate for integrated assessment models, Energy Econ., 64, 552–567, https://doi.org/10.1016/j.eneco.2016.11.015, 2017.

https://doi.org/10.5194/egusphere-2026-1919
Preprint. Discussion started: 26 May 2026

Flores, F., Feijoo, F., DeStephano, P., Herc, L., Pfeifer, A., and Duić, N.: Assessment of the impacts of renewable energy variability in long-term decarbonization strategies, Appl. Energy, 368, 123464, https://doi.org/10.1016/j.apenergy.2024.123464, 2024.

Fu, X., Cheng, J., Peng, L., Zhou, M., Tong, D., and Mauzerall, D. L.: Co-benefits of transport demand reductions from compact urban development in Chinese cities, Nat. Sustain., 7, 294–304, https://doi.org/10.1038/s41893-024-01271-4, 2024.

Fuhrman, J., McJeon, H., Patel, P., Doney, S. C., Shobe, W. M., and Clarens, A. F.: Food–energy–water implications of negative emissions technologies in a +1.5 °C future, Nat. Clim. Change, 10, 920–927, https://doi.org/10.1038/s41558-020-0876-z, 2020.

Fuhrman, J., Bergero, C., Weber, M., Monteith, S., Wang, F. M., Clarens, A. F., Doney, S. C., Shobe, W., and McJeon, H.: Diverse carbon dioxide removal approaches could reduce impacts on the energy–water–land system, Nat. Clim. Change, 13, 341–350, https://doi.org/10.1038/s41558-023-01604-9, 2023.

Fujimori, S., Krey, V., van Vuuren, D., Oshiro, K., Sugiyama, M., Chunark, P., Limmeechokchai, B., Mittal, S., Nishiura, O., Park, C., Rajbhandari, S., Silva Herran, D., Tu, T. T., Zhao, S., Ochi, Y., Shukla, P. R., Masui, T., Nguyen, P. V. H., Cabardos, A.-M., and Riahi, K.: A framework for national scenarios with varying emission reductions, Nat. Clim. Change, 11, 472–480, https://doi.org/10.1038/s41558-021-01048-z, 2021.

Fujimori, S., Wu, W., Doelman, J., Frank, S., Hristov, J., Kyle, P., Sands, R., Van Zeist, W.-J., Havlik, P., Domínguez, I. P., Sahoo, A., Stehfest, E., Tabeau, A., Valin, H., Van Meijl, H., Hasegawa, T., and Takahashi, K.: Land-based climate change mitigation measures can affect agricultural markets and food security, Nat. Food, 3, 110–121, https://doi.org/10.1038/s43016-022-00464-4, 2022.

Girod, B., van Vuuren, D. P., Grahn, M., Kitous, A., Kim, S. H., and Kyle, P.: Climate impact of transportation A model comparison, Clim. Change, 118, 595–608, https://doi.org/10.1007/s10584-012-0663-6, 2013.

Graham, N. T., Iyer, G., Hejazi, M. I., Kim, S. H., Patel, P., and Binsted, M.: Agricultural impacts of sustainable water use in the United States, Sci. Rep., 11, 17917, https://doi.org/10.1038/s41598-021-96243-5, 2021.

Harmsen, M., Kriegler, E., Van Vuuren, D. P., Van Der Wijst, K.-I., Luderer, G., Cui, R., Dessens, O., Drouet, L., Emmerling, J., Morris, J. F., Fosse, F., Fragkiadakis, D., Fragkiadakis, K., Fragkos, P., Fricko, O., Fujimori, S., Gernaat, D., Guivarch, C., Iyer, G., Karkatsoulis, P., Keppo, I., Keramidas, K., Köberle, A., Kolp, P., Krey, V., Krüger, C., Leblanc, F., Mittal, S., Paltsev, S., Rochedo, P., Van Ruijven, B. J., Sands, R. D., Sano, F., Strefler, J., Arroyo, E. V., Wada, K., and Zakeri, B.: Integrated assessment model diagnostics: key indicators and model evolution, Environ. Res. Lett., 16, 054046, https://doi.org/10.1088/1748-9326/abf964, 2021.

Hassan Niazi: gcam-australia, 2025.

Hoesly, R. M., Smith, S. J., Feng, L., Klimont, Z., Janssens-Maenhout, G., Pitkanen, T., Seibert, J. J., Vu, L., Andres, R. J., Bolt, R. M., Bond, T. C., Dawidowski, L., Kholod, N., Kurokawa, J.-I., Li, M., Liu, L., Lu, Z., Moura, M. C. P., O'Rourke, P. R., and Zhang, Q.: Historical (1750–2014) anthropogenic emissions of reactive gases and aerosols from the Community Emissions Data System (CEDS), Geosci. Model Dev., 11, 369–408, https://doi.org/10.5194/gmd-11-369-2018, 2018.

Huang, X., Srikrishnan, V., Lamontagne, J., Keller, K., and Peng, W.: Effects of global climate mitigation on regional air quality and health, Nat. Sustain., 6, 1054–1066, https://doi.org/10.1038/s41893-023-01133-5, 2023.

https://doi.org/10.5194/egusphere-2026-1919
Preprint. Discussion started: 26 May 2026

Huang, Z., Hejazi, M., Li, X., Tang, Q., Vernon, C., Leng, G., Liu, Y., Döll, P., Eisner, S., Gerten, D., Hanasaki, N., and Wada, Y.: Reconstruction of global gridded monthly sectoral water withdrawals for 1971–2010 and analysis of their spatiotemporal patterns, Hydrol. Earth Syst. Sci., 22, 2117–2133, https://doi.org/10.5194/hess-22-2117-2018, 2018.

Hultman, N. E., Clarke, L., Frisch, C., Kennedy, K., McJeon, H., Cyrs, T., Hansel, P., Bodnar, P., Manion, M., Edwards, M. R., Cui, R., Bowman, C., Lund, J., Westphal, M. I., Clapper, A., Jaeger, J., Sen, A., Lou, J., Saha, D., Jaglom, W., Calhoun, K., Igusky, K., deWeese, J., Hammoud, K., Altimirano, J. C., Dennis, M., Henderson, C., Zwicker, G., and O'Neill, J.: Fusing subnational with national climate action is central to decarbonization: the case of the United States, Nat. Commun., 11, 5255, https://doi.org/10.1038/s41467-020-18903-w, 2020.

Intergovernmental Panel on Climate Change (IPCC): Global Warming of 1.5°C: IPCC Special Report on Impacts of Global Warming of 1.5°C above Pre-industrial Levels in Context of Strengthening Response to Climate Change, Sustainable Development, and Efforts to Eradicate Poverty, Cambridge University Press, Cambridge, https://doi.org/10.1017/9781009157940, 2022.

Shared Socioeconomic Pathways Scenario Database (SSP): https://iiasa.ac.at/models-tools-data/ssp, last access: 28 March 2026.

International Monetary Fund: World Economic Outlook, 2021.

Iyer, G., Ledna, C., Clarke, L., Edmonds, J., McJeon, H., Kyle, P., and Williams, J. H.: Measuring progress from nationally determined contributions to mid-century strategies, Nat. Clim. Change, 7, 871–874, https://doi.org/10.1038/s41558-017-0005-9, 2017.

Javadi, P., O'Rourke, P., Fuhrman, J., McJeon, H., Doney, S. C., Shobe, W., and Clarens, A. F.: The impact of regional resources and technology availability on carbon dioxide removal potential in the United States, Environ. Res. Energy, 1, 045007, https://doi.org/10.1088/2753-3751/ad81fb, 2024.

Jeon, S., Roh, M., Oh, J., and Kim, S.: Development of an Integrated Assessment Model at Provincial Level: GCAM-Korea, Energies, 13, 2565, https://doi.org/10.3390/en13102565, 2020.

Jeon, S., Roh, M., and Kim, S.: The derivation of sectoral and provincial implications from power sector scenarios using an integrated assessment model at Korean provincial level: GCAM-Korea, Energy Strategy Rev., 38, 100694, https://doi.org/10.1016/j.esr.2021.100694, 2021a.

Jeon, S., Roh, M., and Kim, S.: The derivation of sectoral and provincial implications from power sector scenarios using an integrated assessment model at Korean provincial level: GCAM-Korea, Energy Strategy Rev., 38, 100694, https://doi.org/10.1016/j.esr.2021.100694, 2021b.

Joint Global Change Research Institute (JGCRI): GCAM v8.2 Documentation: External Inputs for Modeling the Economy, 2026a.

Joint Global Change Research Institute (JGCRI): GCAM v8.2 Documentation: GCAM-USA, 2026b.

Joint Global Change Research Institute (JGCRI): GCAM v8.2 Documentation: Marketplace, 2026c.

Kamboj, P., Hejazi, M., Qiu, Y., Kyle, P., and Iyer, G.: The path to 2060: Saudi Arabia's long-term pathway for GHG emission reduction, Energy Strategy Rev., 55, 101537, https://doi.org/10.1016/j.esr.2024.101537, 2024.

Kang, Y., Fu, L., and Liu, A.: China Statistical Yearbook 2022, China Statistics Press, 2022.

https://doi.org/10.5194/egusphere-2026-1919
Preprint. Discussion started: 26 May 2026

Kholod, N. and Evans, M.: Reducing black carbon emissions from diesel vehicles in Russia: An assessment and policy recommendations, Environ. Sci. Policy, 56, 1–8, https://doi.org/10.1016/j.envsci.2015.10.017, 2016.

Kholod, N., Evans, M., Khan, Z., Hejazi, M., and Chaturvedi, V.: Water-energy-food nexus in India: A critical review, Energy Clim. Change, 2, 100060, https://doi.org/10.1016/j.egycc.2021.100060, 2021.

Kim, H., Qiu, Y., McJeon, H., Clarens, A., Javadi, P., Wang, C., Wang, R., Wang, J., Jiang, H., Miller, A., Cui, R., Behrendt, J., Ou, Y., Yu, S., and Fuhrman, J.: Provincial-scale assessment of direct air capture to meet China's climate neutrality goal under limited bioenergy supply, Environ. Res. Lett., 19, 114021, https://doi.org/10.1088/1748-9326/ad77e7, 2024.

Kim, S. H., Hejazi, M., Liu, L., Calvin, K., Clarke, L., Edmonds, J., Kyle, P., Patel, P., Wise, M., and Davies, E.: Balancing global water availability and use at basin scale in an integrated assessment model, Clim. Change, 136, 217–231, https://doi.org/10.1007/s10584-016-1604-6, 2016.

Kyle, P. and Kim, S. H.: Long-term implications of alternative light-duty vehicle technologies for global greenhouse gas emissions and primary energy demands, Energy Policy, 39, 3012–3024, https://doi.org/10.1016/j.enpol.2011.03.016, 2011.

Kyle, P., Hejazi, M., Kim, S., Patel, P., Graham, N., and Liu, Y.: Assessing the future of global energy-for-water, Environ. Res. Lett., 16, 024031, https://doi.org/10.1088/1748-9326/abd8a9, 2021.

Li, J., Lin, J., Wang, J., Lu, X., Nielsen, C. P., McElroy, M. B., Song, Y., Song, J., Lyu, X., Yu, M., Wu, S., and Yu, Z.: Redesigning electrification of China's ammonia and methanol industry to balance decarbonization with power system security, Nat. Energy, 10, 762–773, https://doi.org/10.1038/s41560-025-01779-9, 2025.

Liu, Y., Tong, D., Cheng, J., Davis, S. J., Yu, S., Yarlagadda, B., Clarke, L. E., Brauer, M., Cohen, A. J., Kan, H., Xue, T., and Zhang, Q.: Role of climate goals and clean-air policies on reducing future air pollution deaths in China: a modelling study, Lancet Planet. Health, 6, e92–e99, https://doi.org/10.1016/S2542-5196(21)00326-0, 2022.

Lou, J., Yu, S., Cui, R. Y., Miller, A., and Hultman, N.: A provincial analysis on wind and solar investment needs towards China's carbon neutrality, Appl. Energy, 378, 124841, https://doi.org/10.1016/j.apenergy.2024.124841, 2025.

Lu, X., Chen, S., Nielsen, C. P., Zhang, C., Li, J., Xu, H., Wu, Y., Wang, S., Song, F., Wei, C., He, K., McElroy, M. B., and Hao, J.: Combined solar power and storage as cost-competitive and grid-compatible supply for China's future carbon-neutral electricity system, Proc. Natl. Acad. Sci., 118, e2103471118, https://doi.org/10.1073/pnas.2103471118, 2021.

Luo, H., Peng, W., Fawcett, A., Green, J. F., Iyer, G., Meckling, J., Nahm, J., and Victor, D. G.: Modelling the impacts of policy sequencing on energy decarbonization, Nat. Clim. Change, https://doi.org/10.1038/s41558-025-02497-6, 2025.

Ma, X., Peng, T., Wang, T., Zhang, Y., Shao, T., and Pan, X.: Carbon assets alone are insufficient to sustain China's agroforestry biomass power generation, Cell Rep. Sustain., 2, 100410, https://doi.org/10.1016/j.crsus.2025.100410, 2025.

Macknick, J., Newmark, R., Heath, G., and Hallett, K. C.: Operational water consumption and withdrawal factors for electricity generating technologies: a review of existing literature, Environ. Res. Lett., 7, 045802, https://doi.org/10.1088/1748-9326/7/4/045802, 2012.

Matthew Binsted, Russell Horowitz, and Harrison Suchyta: Core Model Proposal #373: Add Exogenous Shutdown Decider, Joint Global Change Research Institute, 2023.

https://doi.org/10.5194/egusphere-2026-1919
Preprint. Discussion started: 26 May 2026

McCollum, D. L., Wilson, C., Pettifor, H., Ramea, K., Krey, V., Riahi, K., Bertram, C., Lin, Z., Edelenbosch, O. Y., and Fujisawa, S.: Improving the behavioral realism of global integrated assessment models: An application to consumers' vehicle choices, Transp. Res. Part Transp. Environ., 55, 322–342, https://doi.org/10.1016/j.trd.2016.04.003, 2017.

Mcfadden, D. L.: Conditional Logit Analysis of Qualitative Choice Behavior, Frontiers in Econometrics, 1974.

Mi, Z. and Sun, X.: Provinces with transitions in industrial structure and energy mix performed best in climate change mitigation in China, Commun. Earth Environ., 2, 182, https://doi.org/10.1038/s43247-021-00258-9, 2021.

Ministry of Water Resources of the People's Republic of China: China's Water Resources Bulletin, 2021.

Mishra, G. S., Kyle, P., Teter, J., Morrison, G. M., Kim, S. H., and Yeh, S.: Transportation Module of Global Change Assessment Model (GCAM): Model Documentation- Version 1.0, 2013.

Mongird, K., Bracken, C., Burleyson, C. D., Oikonomou, K., Ou, Y., Rice, J. S., Thurber, T., and Voisin, N.: More land is needed for solar and wind infrastructure under a high renewables scenario in the Western US by 2050, Commun. Earth Environ., 6, 765, https://doi.org/10.1038/s43247-025-02632-3, 2025.

Morrow, D. R., Apeaning, R., and Guard, G.: GCAM-CDR v1.0: enhancing the representation of carbon dioxide removal technologies and policies in an integrated assessment model, Geosci. Model Dev., 16, 1105–1118, https://doi.org/10.5194/gmd-16-1105-2023, 2023.

Muratori, M., Ledna, C., McJeon, H., Kyle, P., Patel, P., Kim, S. H., Wise, M., Kheshgi, H. S., Clarke, L. E., and Edmonds, J.: Cost of power or power of cost: A U.S. modeling perspective, Renew. Sustain. Energy Rev., 77, 861–874, https://doi.org/10.1016/j.rser.2017.04.055, 2017a.

Muratori, M., Smith, S. J., Kyle, P., Link, R., Mignone, B. K., and Kheshgi, H. S.: Role of the Freight Sector in Future Climate Change Mitigation Scenarios, Environ. Sci. Technol., 51, 3526–3533, https://doi.org/10.1021/acs.est.6b04515, 2017b.

Narayan, K. B., O'Neill, B. C., Waldhoff, S. T., and Tebaldi, C.: Non-parametric projections of national income distribution consistent with the Shared Socioeconomic Pathways, Environ. Res. Lett., 18, 044013, https://doi.org/10.1088/1748-9326/acbdb0, 2023.

National Bureau of Statistics: China Statistical Yearbook 2016, China Statistical Press, 2016.

National Bureau of Statistics of China: China Compendium of 60-year Statistics, 2009.

National Bureau of Statistics of China: China Statistical Yearbook, 2020.

National Bureau of Statistics of China: Annual National Sample Survey of Population, 2022.

National Bureau of Statistics of China: China Industrial Statistical Yearbook, 2026.

O'Neill, B. C., Kriegler, E., Riahi, K., Ebi, K. L., Hallegatte, S., Carter, T. R., Mathur, R., and Van Vuuren, D. P.: A new scenario framework for climate change research: the concept of shared socioeconomic pathways, Clim. Change, 122, 387–400, https://doi.org/10.1007/s10584-013-0905-2, 2014.

Ou, Y., West, J. J., Smith, S. J., Nolte, C. G., and Loughlin, D. H.: Air pollution control strategies directly limiting national health damages in the US, Nat. Commun., 11, 957, https://doi.org/10.1038/s41467-020-14783-2, 2020.

https://doi.org/10.5194/egusphere-2026-1919
Preprint. Discussion started: 26 May 2026

Ou, Y., Iyer, G., Clarke, L., Edmonds, J., Fawcett, A. A., Hultman, N., McFarland, J. R., Binsted, M., Cui, R., Fyson, C., Geiges, A., Gonzales-Zuñiga, S., Gidden, M. J., Höhne, N., Jeffery, L., Kuramochi, T., Lewis, J., Meinshausen, M., Nicholls, Z., Patel, P., Ragnauth, S., Rogelj, J., Waldhoff, S., Yu, S., and McJeon, H.: Can updated climate pledges limit warming well below 2°C?, Science, 374, 693–695, https://doi.org/10.1126/science.abl8976, 2021a.

Ou, Y., Kittner, N., Babaee, S., Smith, S. J., Nolte, C. G., and Loughlin, D. H.: Evaluating long-term emission impacts of large-scale electric vehicle deployment in the US using a human-Earth systems model, Appl. Energy, 300, 117364, https://doi.org/10.1016/j.apenergy.2021.117364, 2021b.

Ou, Y., Binsted, M., Iyer, G., Patel, P., and Wise, M.: US state-level capacity expansion pathways with improved modeling of the power sector dynamics within a multisector model, Energy Strategy Rev., 38, 100739, https://doi.org/10.1016/j.esr.2021.100739, 2021c.

Paladugula, A. L., Kholod, N., Chaturvedi, V., Ghosh, P. P., Pal, S., Clarke, L., Evans, M., Kyle, P., Koti, P. N., Parikh, K., Qamar, S., and Wilson, S. A.: A multi-model assessment of energy and emissions for India's transportation sector through 2050, Energy Policy, 116, 10–18, https://doi.org/10.1016/j.enpol.2018.01.037, 2018.

Pan, X., Chen, W., Wang, L., Lin, L., and Li, N.: The role of biomass in China's long-term mitigation toward the Paris climate goals, Environ. Res. Lett., 13, 124028, https://doi.org/10.1088/1748-9326/aaf06c, 2018.

Pan, X., Ma, X., Zhang, Y., Shao, T., Peng, T., Li, X., Wang, L., and Chen, W.: Implications of carbon neutrality for power sector investments and stranded coal assets in China, Energy Econ., 121, 106682, https://doi.org/10.1016/j.eneco.2023.106682, 2023.

Peng, K., Feng, K., Chen, B., Shan, Y., Zhang, N., Wang, P., Fang, K., Bai, Y., Zou, X., Wei, W., Geng, X., Zhang, Y., and Li, J.: The global power sector's low-carbon transition may enhance sustainable development goal achievement, Nat. Commun., 14, 3144, https://doi.org/10.1038/s41467-023-38987-4, 2023.

Peng, W., Iyer, G., Binsted, M., Marlon, J., Clarke, L., Edmonds, J. A., and Victor, D. G.: The surprisingly inexpensive cost of state-driven emission control strategies, Nat. Clim. Change, 11, 738–745, https://doi.org/10.1038/s41558-021-01128-0, 2021.

Qin, Y., Zhou, M., Hao, Y., Huang, X., Tong, D., Huang, L., Zhang, C., Cheng, J., Gu, W., Wang, L., He, X., Zhou, D., Chen, Q., Ding, A., and Zhu, T.: Amplified positive effects on air quality, health, and renewable energy under China's carbon neutral target, Nat. Geosci., 17, 411–418, https://doi.org/10.1038/s41561-024-01425-1, 2024.

Rao, N. D., Sauer, P., Gidden, M., and Riahi, K.: Income inequality projections for the Shared Socioeconomic Pathways (SSPs), Futures, 105, 27–39, https://doi.org/10.1016/j.futures.2018.07.001, 2019.

Roelfsema, M., van Soest, H. L., Harmsen, M., van Vuuren, D. P., Bertram, C., den Elzen, M., Höhne, N., Iacobuta, G., Krey, V., Kriegler, E., Luderer, G., Riahi, K., Ueckerdt, F., Després, J., Drouet, L., Emmerling, J., Frank, S., Fricko, O., Gidden, M., Humpenöder, F., Huppmann, D., Fujimori, S., Fragkiadakis, K., Gi, K., Keramidas, K., Köberle, A. C., Aleluia Reis, L., Rochedo, P., Schaeffer, R., Oshiro, K., Vrontisi, Z., Chen, W., Iyer, G. C., Edmonds, J., Kannavou, M., Jiang, K., Mathur, R., Safonov, G., and Vishwanathan, S. S.: Taking stock of national climate policies to evaluate implementation of the Paris Agreement, Nat. Commun., 11, 2096, https://doi.org/10.1038/s41467-020-15414-6, 2020.

Sampedro, J., Iyer, G., Msangi, S., Waldhoff, S., Hejazi, M., and Edmonds, J. A.: Implications of different income distributions for future residential energy demand in the US, Environ. Res. Lett., 17, 014031, 2022.

https://doi.org/10.5194/egusphere-2026-1919
Preprint. Discussion started: 26 May 2026

Sampedro, J., Waldhoff, S. T., Edmonds, J. A., Iyer, G., Msangi, S., Narayan, K. B., Patel, P., and Wise, M.: Residential energy demand, emissions, and expenditures at regional and income-decile level for alternative futures, Environ. Res. Lett., 19, 084031, https://doi.org/10.1088/1748-9326/ad6015, 2024.

Sampedro, J., Horowitz, R., Rodés-Bachs, C., and Van De Ven, D.-J.: GCAM-Europe v7.2.0: Enhancing Policy-Relevant Climate Modelling Through Spatial and Sectoral Detail, https://doi.org/10.5194/egusphere-2025-3546, 11 August 2025.

Schaeffer, R., Köberle, A., van Soest, H. L., Bertram, C., Luderer, G., Riahi, K., Krey, V., van Vuuren, D. P., Kriegler, E., Fujimori, S., Chen, W., He, C., Vrontisi, Z., Vishwanathan, S., Garg, A., Mathur, R., Shekhar, S., Oshiro, K., Ueckerdt, F., Safonov, G., Iyer, G., Gi, K., and Potashnikov, V.: Comparing transformation pathways across major economies, Clim. Change, 162, 1787–1803, https://doi.org/10.1007/s10584-020-02837-9, 2020.

Selin, N. E., Giang, A., and Clark, W. C.: Progress in modeling dynamic systems for sustainable development, Proc. Natl. Acad. Sci., 120, e2216656120, https://doi.org/10.1073/pnas.2216656120, 2023.

Shao, T., Peng, T., Zhu, L., Lu, Y., Wang, L., and Pan, X.: China's transportation decarbonization in the context of carbon neutrality: A segment-mode analysis using integrated modelling, Environ. Impact Assess. Rev., 105, 107392, https://doi.org/10.1016/j.eiar.2023.107392, 2024.

Shao, T., Pan, X., Wang, L., Xiong, W., Wang, T., and Song, J.: Assessing CCS development uncertainties in China's energy system aligned with carbon neutrality, Appl. Energy, 399, 126545, https://doi.org/10.1016/j.apenergy.2025.126545, 2025.

Shi, W., Ou, Y., Smith, S. J., Ledna, C. M., Nolte, C. G., and Loughlin, D. H.: Projecting state-level air pollutant emissions using an integrated assessment model: GCAM-USA, Appl. Energy, 208, 511–521, https://doi.org/10.1016/j.apenergy.2017.09.122, 2017.

Speizer, S., Fuhrman, J., Aldrete Lopez, L., George, M., Kyle, P., Monteith, S., and McJeon, H.: Integrated assessment modeling of a zero-emissions global transportation sector, Nat. Commun., 15, 4439, https://doi.org/10.1038/s41467-024-48424-9, 2024.

Sun, Y., Jiang, Y., Xing, J., Ou, Y., Wang, S., Loughlin, D. H., Yu, S., Ren, L., Li, S., Dong, Z., Zheng, H., Zhao, B., Ding, D., Zhang, F., Zhang, H., Song, Q., Liu, K., Klimont, Z., Woo, J.-H., Lu, X., Li, S., and Hao, J.: Air Quality, Health, and Equity Benefits of Carbon Neutrality and Clean Air Pathways in China, Environ. Sci. Technol., 58, 15027–15037, https://doi.org/10.1021/acs.est.3c10076, 2024.

Thomson, A. M., Calvin, K. V., Smith, S. J., Kyle, G. P., Volke, A., Patel, P., Delgado-Arias, S., Bond-Lamberty, B., Wise, M. A., Clarke, L. E., and Edmonds, J. A.: RCP4.5: a pathway for stabilization of radiative forcing by 2100, Clim. Change, 109, 77–94, https://doi.org/10.1007/s10584-011-0151-4, 2011.

Tong, D., Cheng, J., Liu, Y., Yu, S., Yan, L., Hong, C., Qin, Y., Zhao, H., Zheng, Y., Geng, G., Li, M., Liu, F., Zhang, Y., Zheng, B., Clarke, L., and Zhang, Q.: Dynamic projection of anthropogenic emissions in China: methodology and 2015–2050 emission pathways under a range of socio-economic, climate policy, and pollution control scenarios, Atmospheric Chem. Phys., 20, 5729–5757, https://doi.org/10.5194/acp-20-5729-2020, 2020.

Tong, D., Farnham, D. J., Duan, L., Zhang, Q., Lewis, N. S., Caldeira, K., and Davis, S. J.: Geophysical constraints on the reliability of solar and wind power worldwide, Nat. Commun., 12, 6146, https://doi.org/10.1038/s41467-021-26355-z, 2021.

https://doi.org/10.5194/egusphere-2026-1919
Preprint. Discussion started: 26 May 2026

Turner, S. W. D., Hejazi, M., Yonkofski, C., Kim, S. H., and Kyle, P.: Influence of Groundwater Extraction Costs and Resource Depletion Limits on Simulated Global Nonrenewable Water Withdrawals Over the Twenty-First Century, Earths Future, 7, 123–135, https://doi.org/10.1029/2018EF001105, 2019.

Van Ruijven, B. J., Van Vuuren, D. P., Boskaljon, W., Neelis, M. L., Saygin, D., and Patel, M. K.: Long-term model-based projections of energy use and CO2 emissions from the global steel and cement industries, Resour. Conserv. Recycl., 112, 15–36, https://doi.org/10.1016/j.resconrec.2016.04.016, 2016.

van Vuuren, D., O'Neill, B., Tebaldi, C., Chini, L., Friedlingstein, P., Hasegawa, T., Riahi, K., Sanderson, B., Govindasamy, B., Bauer, N., Eyring, V., Fall, C., Frieler, K., Gidden, M., Gohar, L., Jones, A., King, A., Knutti, R., Kriegler, E., Lawrence, P., Lennard, C., Lowe, J., Mathison, C., Mehmood, S., Prado, L., Zhang, Q., Rose, S., Ruane, A., Schleussner, C.-F., Seferian, R., Sillmann, J., Smith, C., Sörensson, A., Panickal, S., Tachiiri, K., Vaughan, N., Vishwanathan, S., Yokohata, T., and Ziehn, T.: The Scenario Model Intercomparison Project for CMIP7 (ScenarioMIP-CMIP7), EGUsphere, 2025, 1–38, https://doi.org/10.5194/egusphere-2024-3765, 2025.

Wang, B., Xu, S., Wang, Z., Shan, Y., Zhang, B., Li, H., Deng, N., and Shi, H.: Retrofitting Coal Power Units with Biomass and Coal Cofiring Intensifies Air Pollution and Health Risks, Environ. Sci. Technol., 58, 21523–21535, https://doi.org/10.1021/acs.est.4c04122, 2024.

Wang, B., Nie, F., Wang, Z., Ou, Y., and Deng, N.: Systemic Risks of Excessive CCS Deployment in Power-Sector Decarbonization, Environ. Sci. Technol., https://doi.org/10.1021/acs.est.5c10957, 2025a.

Wang, H., Liu, Y., Wu, F., Dai, H., Duan, H., Guo, F., Hultman, N., Lu, X., McJeon, H., Miller, A., Tong, D., Yu, S., Yuan, W., Zhang, D., Cui, R., Zhang, Q., and Ou, Y.: Bridging China's Climate Targets and Mitigation Capacity through Sectoral Policy Implementation, Environ. Sci. Technol., https://doi.org/10.1021/acs.est.5c11232, 2026.

Wang, J., Lu, X., Wang, H., Ou, Y., Wang, J., Tong, D., Li, Y., Ruan, Z., Yin, Z., Zhou, W., McLellan, B., Xing, E., MacLennan, A. M., Fan, J., Zhang, X., McElroy, M. B., and He, K.: Reassessing immediate coal phase-out: Dual imperatives of capacity control and renewables expansion in China's net-zero strategy, Nexus, 2, 100081, https://doi.org/10.1016/j.ynexs.2025.100081, 2025b.

Wang, J., Lu, X., Wang, H., Ou, Y., Wang, J., Tong, D., Li, Y., Ruan, Z., Yin, Z., Zhou, W., McLellan, B., Xing, E., MacLennan, A. M., Fan, J., Zhang, X., McElroy, M. B., and He, K.: Reassessing immediate coal phase-out: Dual imperatives of capacity control and renewables expansion in China's net-zero strategy, Nexus, 2, https://doi.org/10.1016/j.ynexs.2025.100081, 2025c.

Wang, L., Patel, P. L., Yu, S., Liu, B., McLeod, J., Clarke, L. E., and Chen, W.: Win–Win strategies to promote air pollutant control policies and non-fossil energy target regulation in China, Appl. Energy, 163, 244–253, https://doi.org/10.1016/j.apenergy.2015.10.189, 2016.

Wang, Z., Zhang, H., Wang, B., Li, H., Ma, J., Zhang, B., Zhuge, C., and Shan, Y.: Trade-Offs between Direct Emission Reduction and Intersectoral Additional Emissions: Evidence from the Electrification Transition in China's Transport Sector, Environ. Sci. Technol., 57, 11389–11400, https://doi.org/10.1021/acs.est.3c00556, 2023a.

Wang, Z., Li, H., Zhang, B., Wang, B., Li, H., Tian, X., Lin, J., and Feng, W.: Unequal residential heating burden caused by combined heat and power phase-out under climate goals, Nat. Energy, 8, 881–890, https://doi.org/10.1038/s41560-023-01308-6, 2023b.

Wolfram, C., Shelef, O., and Gertler, P.: How Will Energy Demand Develop in the Developing World?, J. Econ. Perspect., 26, 119–38, https://doi.org/10.1257/jep.26.1.119, 2012.

https://doi.org/10.5194/egusphere-2026-1919
Preprint. Discussion started: 26 May 2026

Wu, T., Wang, S., Wang, L., and Tang, X.: Contribution of China's online car-hailing services to its 2050 carbon target: Energy consumption assessment based on the GCAM-SE model, Energy Policy, 160, 112714, https://doi.org/10.1016/j.enpol.2021.112714, 2022.

Xing, J., Lu, X., Wang, S., Wang, T., Ding, D., Yu, S., Shindell, D., Ou, Y., Morawska, L., Li, S., Ren, L., Zhang, Y., Loughlin, D., Zheng, H., Zhao, B., Liu, S., Smith, K. R., and Hao, J.: The quest for improved air quality may push China to continue its CO2 reduction beyond the Paris Commitment, Proc. Natl. Acad. Sci., 117, 29535–29542, https://doi.org/10.1073/pnas.2013297117, 2020.

Yarlagadda, B., Wild, T., Zhao, X., Clarke, L., Cui, R., Khan, Z., Birnbaum, A., and Lamontagne, J.: Trade and Climate Mitigation Interactions Create Agro-Economic Opportunities With Social and Environmental Trade-Offs in Latin America and the Caribbean, Earths Future, 11, https://doi.org/10.1029/2022EF003063, 2023.

Yeh, S., Mishra, G. S., Fulton, L., Kyle, P., McCollum, D. L., Miller, J., Cazzola, P., and Teter, J.: Detailed assessment of global transport-energy models' structures and projections, Transp. Res. Part Transp. Environ., 55, 294–309, https://doi.org/10.1016/j.trd.2016.11.001, 2017.

Yin, X., Chen, W., Eom, J., Clarke, L. E., Kim, S. H., Patel, P. L., Yu, S., and Kyle, G. P.: China's transportation energy consumption and CO2 emissions from a global perspective, Energy Policy, 82, 233–248, https://doi.org/10.1016/j.enpol.2015.03.021, 2015a.

Yin, X., Chen, W., Eom, J., Clarke, L. E., Kim, S. H., Patel, P. L., Yu, S., and Kyle, G. P.: China's transportation energy consumption and CO2 emissions from a global perspective, Energy Policy, 82, 233–248, https://doi.org/10.1016/j.enpol.2015.03.021, 2015b.

Yin, Z., Lu, X., Nielsen, C. P., Cui, R. Y., Ou, Y., Han, M., Shi, M., Ruan, Z., Wang, J., Su, Y., Zhang, C., Bian, S., Xing, E., Zhou, W., Li, J., McElroy, M. B., and He, K.: Mitigating inequity risks in China's net-zero energy transition via an enhanced renewable-guided industrial spatial reconfiguration, The Innovation, https://doi.org/10.1016/j.xinn.2026.101308, 2026.

Younis, O., Davies, E. G. R., Chiappori, D. V., Binsted, M., Siddiqui, M.-S., Arbuckle, E. J., and Macaluso, N.: Exploring water use pathways under deep decarbonization scenarios in Canada at subnational scales using GCAM-Canada, J. Environ. Manage., 391, 126416, https://doi.org/10.1016/j.jenvman.2025.126416, 2025a.

Younis, O., Davies, E. G. R., Chiappori, D. V., Binsted, M., Siddiqui, M.-S., Arbuckle, E. J., and Macaluso, N.: Exploring water use pathways under deep decarbonization scenarios in Canada at subnational scales using GCAM-Canada, J. Environ. Manage., 391, 126416, https://doi.org/10.1016/j.jenvman.2025.126416, 2025b.

Yu, S., Eom, J., Evans, M., and Clarke, L.: A long-term, integrated impact assessment of alternative building energy code scenarios in China, Energy Policy, 67, 626–639, https://doi.org/10.1016/j.enpol.2013.11.009, 2014a.

Yu, S., Eom, J., Zhou, Y., Evans, M., and Clarke, L.: Scenarios of building energy demand for China with a detailed regional representation, Energy, 67, 284–297, https://doi.org/10.1016/j.energy.2013.12.072, 2014b.

Yu, S., Horing, J., Liu, Q., Dahowski, R., Davidson, C., Edmonds, J., Liu, B., Mcjeon, H., McLeod, J., Patel, P., and Clarke, L.: CCUS in China's mitigation strategy: insights from integrated assessment modeling, Int. J. Greenh. Gas Control, 84, 204–218, https://doi.org/10.1016/j.ijggc.2019.03.004, 2019.

Yu, S., Yarlagadda, B., Siegel, J. E., Zhou, S., and Kim, S.: The role of nuclear in China's energy future: Insights from integrated assessment, Energy Policy, 139, 111344, https://doi.org/10.1016/j.enpol.2020.111344, 2020.

https://doi.org/10.5194/egusphere-2026-1919
Preprint. Discussion started: 26 May 2026

Yu, Y., You, K., Cai, W., Feng, W., Li, R., Liu, Q., Chen, L., and Liu, Y.: City-level building operation and end-use carbon emissions dataset from China for 2015–2020, Sci. Data, 11, 138, https://doi.org/10.1038/s41597-024-02971-4, 2024.

Zhang, A., Gao, J., Quan, J., Zhou, B., Lam, S. K., Zhou, Y., Lin, E., Jiang, K., Clarke, L. E., Zhang, X., Yu, S., Kyle, G. P., Li, H., Zhou, S., Gao, S., Wang, W., and Guan, Y.: The implications for energy crops under China's climate change challenges, Energy Econ., 96, 105103, https://doi.org/10.1016/j.eneco.2021.105103, 2021.

Zhang, Q., Wang, L., Chen, W., and Zhang, C.: Assessing the impact of hydrogen trade towards low-carbon energy transition, Appl. Energy, 376, 124233, https://doi.org/10.1016/j.apenergy.2024.124233, 2024a.

Zhang, Q., Wang, L., Chen, W., and Zhang, C.: Assessing the impact of hydrogen trade towards low-carbon energy transition, Appl. Energy, 376, 124233, https://doi.org/10.1016/j.apenergy.2024.124233, 2024b.

Zhang, Q.-Z., Wang, L.-N., Chen, W.-Y., Zhang, C.-L., Xiang, K.-L., and Chen, J.-Y.: Analysis of hydrogen supply and demand in China's energy transition towards carbon neutrality, Adv. Clim. Change Res., 15, 924–935, https://doi.org/10.1016/j.accre.2024.07.013, 2024c.

Zhang, X.: Underground data centers as urban energy infrastructure, Nat. Cities, 3, 194–195, https://doi.org/10.1038/s44284-026-00406-2, 2026.

Zhang, Y., Ou, Y., Waldhoff, S., O'Neill, B., Iyer, G., Sampedro, J., and Casper, K.: Long-term decarbonization impacts on residential energy security across income groups and US states, Environ. Res. Lett., 20, 054040, https://doi.org/10.1088/1748-9326/adca4c, 2025.

Zheng, B., Zhang, Q., Tong, D., Chen, C., Hong, C., Li, M., Geng, G., Lei, Y., Huo, H., and He, K.: Resolution dependence of uncertainties in gridded emission inventories: a case study in Hebei, China, Atmospheric Chem. Phys., 17, 921–933, https://doi.org/10.5194/acp-17-921-2017, 2017.

Zheng, B., Tong, D., Li, M., Liu, F., Hong, C., Geng, G., Li, H., Li, X., Peng, L., Qi, J., Yan, L., Zhang, Y., Zhao, H., Zheng, Y., He, K., and Zhang, Q.: Trends in China's anthropogenic emissions since 2010 as the consequence of clean air actions, Atmospheric Chem. Phys., 18, 14095–14111, https://doi.org/10.5194/acp-18-14095-2018, 2018.

Zheng, B., Cheng, J., Geng, G., Wang, X., Li, M., Shi, Q., Qi, J., Lei, Y., Zhang, Q., and He, K.: Mapping anthropogenic emissions in China at 1 km spatial resolution and its application in air quality modeling, Sci. Bull., 66, 612–620, https://doi.org/10.1016/j.scib.2020.12.008, 2021.

Zhong, J., Zhang, X., Zhang, D., Wang, D., Guo, L., Peng, H., Huang, X., Wang, Z., Lei, Y., Lu, Y., Qu, C., Zhang, X., and Miao, C.: Plausible global emissions scenario for 2 °C aligned with China's net-zero pathway, Nat. Commun., 16, 8102, https://doi.org/10.1038/s41467-025-62983-5, 2025.

Zhou, F., Bo, Y., Ciais, P., Dumas, P., Tang, Q., Wang, X., Liu, J., Zheng, C., Polcher, J., Yin, Z., Guimberteau, M., Peng, S., Ottle, C., Zhao, X., Zhao, J., Tan, Q., Chen, L., Shen, H., Yang, H., Piao, S., Wang, H., and Wada, Y.: Deceleration of China's human water use and its key drivers, Proc. Natl. Acad. Sci., 117, 7702–7711, https://doi.org/10.1073/pnas.1909902117, 2020.

Zhou, S., Kyle, G. P., Yu, S., Clarke, L. E., Eom, J., Luckow, P., Chaturvedi, V., Zhang, X., and Edmonds, J. A.: Energy use and CO2 emissions of China's industrial sector from a global perspective, Energy Policy, 58, 284–294, https://doi.org/10.1016/j.enpol.2013.03.014, 2013.